

Separation of complex feed streams of products by layer melt crystallization

DISSERTATION

zur Erlangung des

Doktorgrades der Ingenieurwissenschaften (Dr.-Ing.)

des

Zentrums für Ingenieurwissenschaften

der Martin-Luther-Universität

Halle-Wittenberg,

vorgelegt von

Herr. M.Sc. Muhammad Ahmad

geboren am 23. 08. 1983 in Multan, Pakistan

Gutachter: 1. Prof. Dr.-Ing. Dr. h.c. Joachim Ulrich

2. apl. Prof. Dr. rer. nat. Heike Lorenz

Datum der Verteidigung: 11.07.2016

Acknowledgement

First and most importantly, appreciations and praises are for Almighty Allah who gave me the strength and wisdom to complete this task.

It is difficult to overstate my gratitude and best regards to my supervisor, Prof. Dr.-Ing. Dr. h.c. Joachim Ulrich. His extensive knowledge and logical way of thinking have been of great value for me. His understanding, incessant encouragement and personal guidance have provided a good basis for the present thesis. I am really thankful to him for providing me this opportunity and integrate me in his work group where I met wonderful people of different nationalities. I gratefully acknowledge his presence and availability besides his busy schedule for the positive discussions whenever needed, which helped me to complete the work.

I would also like to express deep and sincere gratitude to apl. Prof. Dr. rer. nat. Heike Lorenz for her willingness to be the second reviewer for this work and my special thanks also goes to all the members of the examination committee.

In addition, I want to thank SKW Piesteritz and AIP for being involved in the topic of this work and financially supporting this project. I also acknowledge Prof. Dr. Dr. h.c. Hans Joachim Niclas for the helpful discussions during the project seminars. I am also grateful to Dr. Ute Radics for being a first contact person at SKW Piesteritz and having organized some HPLC measurements in her lab.

Moreover, I would like to express my appreciation for all my former and current TVT colleagues for their continued help and friendly support during my stay especially Sandra and Steffi who helped me a lot during my early days at TVT with their encouraging suggestions and discussions related to the work. I am also grateful to Ronny for helping me in setting up a n HPLC, without which it was impossible to complete this work and Patrick for helping, e.g. with the translation of a summary of my work. Believe me, all of you are the best colleagues, I have worked with so far. Thanks for being a real positive inspiration to me that I believe will accompany me through my future career days.

At the end, I also want to thank our technical assistant Mr. Schütze who helped me for building up different experimental setups necessary for the work and our lab assistant Ms. Höser for conducting GC analysis for me. Special thanks to Ms. Kirchner also for her silent but significant efforts for doing all important official credentials and making all important things ready for us, without bothering anyone.

Many thanks to my students Mauricio, Katherina and Marden for their good lab work which helped me in many different ways.

My deepest gratitude goes to my parents, family and friends for their unagging love and support throughout my life. This dissertation would not have been possible without them. I am, especially, indebted to my mother, for her continual financial and emotional support throughout my study period in Germany.

Finally, a special appreciation goes to my wife for her endless support and never ending encouragement that has always driven me to pursue my goal.

Muhammad Ahmad

Table of Contents

1. Introduction	1
2. State of the art	3
2.1 Melt Crystallization	3
2.1.1 Solid-liquid equilibrium	4
2.1.1.1 Eutectic phase diagram	4
2.1.2 Industrial crystallization techniques	7
2.1.3 Basics of solid layer crystallization	7
2.2 Purification mechanism of industrial layer melt crystallization	9
2.2.1 Crystallization	9
2.2.2 Sweating (partial melting)	10
2.2.3 Total melting	10
2.3 Industrial problems	11
3. Objectives of the work	14
4. Materials and Methods	16
4.1 Materials	16
4.1.1 Raw Product 'A'	16
4.1.2 3-Isomer	16
4.1.3 5-isomer	17
4.1.4 Methanol	17
4.1.5 Acetonitrile	17
4.1.6 Benzoic acid	18
4.2 Experimental methods	18
4.2.1 Solid-Liquid equilibrium	18
4.2.1.1 Differential scanning calorimetry (DSC)	18
4.2.2 Experimental set up for crystallization	19

4.2.2.1	Procedure for experiment.....	21
4.2.2.2	Sweating	22
4.2.2.3	High Performance Liquid Chromatography	22
4.2.2.3.1	HPLC analysis	23
4.2.3	Crystal morphology.....	25
4.2.3.1	Analytical method.....	26
4.2.4	Method for calculating heat of fusion and vaporization	27
5.	Results	29
5.1	Case study I ‘Raw Product ‘A’	29
5.1.1	Solid-liquid equilibrium.....	29
5.1.2	Average layer thickness at different temperatures as a function of crystallization time	32
5.1.3	Crystal growth rate at different temperatures as a function of layer thickness.....	33
5.1.4	Effect of crystallization time on purity of the crystal layer.....	34
5.1.5	Purification by sweating	35
5.1.6	Purification of residual melt.....	37
5.1.7	Crystal shape, habit and morphology	40
5.2	Case study II ‘3-isomer’	41
5.2.1	Solid-liquid equilibrium.....	41
5.2.2	Purity of the layer.....	42
5.2.3	Residual melt treatment.....	43
5.3	Calculation of phase change energies.....	44
5.3.1	Enthalpy of vaporization	44
5.3.1.1	Benzoic acid.....	46
5.3.1.2	Raw Product ‘A’.....	47

5.3.2	Phase change energies	49
6.	Discussion.....	51
6.1	Case study I ‘Raw Product ‘A’.....	51
6.1.1	Solid-liquid equilibrium.....	51
6.1.2	Effect of crystallization time on crystal growth rate at different temperatures	53
6.1.3	Effect of crystallization time on purity of the crystal layer.....	54
6.1.4	Purification by sweating	55
6.1.5	Purification of residual melt.....	57
6.1.6	Yield of the process	58
6.1.7	Crystal Shape, habit and morphology.....	60
6.2	Case study II ‘3-isomer’	60
6.2.1	Solid-liquid equilibrium.....	60
6.2.2	Purity of the layer.....	60
6.3	Energy efficiency of melt crystallization process.....	61
6.4	Process flow diagram	63
7.	Conclusion	65
8.	Summary.....	69
9.	Zusammenfassung	71
10.	List of symbols and abbreviations	74
11.	References.....	76

1. Introduction

From the last few decades, driven by strict governmental policies toward chemicals disposal and emissions, the chemical industries are looking for new innovative separation technologies to overcome all these problems. Melt crystallization can provide a unique solution for high purity applications in addition to environmental and health benefits [Gil91]. Consequently, melt crystallization is also an attractive process from an ecological point of view.

Many materials which have close boiling points like different isomers, azeotropic mixtures and heat sensitive materials which are difficult to be purified by conventional technologies like distillation, liquid extraction and absorption etc., can be separated by melt crystallization [Kim02]. The basic principle of this technique is cooling the melt in a controlled way to crystallize a relative pure crystal fraction [Kön08]. The following advantages of melt crystallization can be seen: (1) high selectivity with high purity in a single step if the mixture is eutectic; (2) no solvents; (3) low-temperature operation compared to distillation; (4) less phase change energy compared to liquid–gas phase transition [Bei12].

In comparison with other separation technologies, e.g. distillation, the energy necessary for the phase change from liquid to solid is much lower. The basis for this comparison is a relatively low heat of fusion as compared to their heat of vaporization. The energy required for the phase transition liquid-solid is only about $1/3^{\text{rd}}$ to $1/7^{\text{th}}$ of the gas-liquid phase transition energy. Due to the low-temperature, it is also possible to treat heat-sensitive substances, like foods or polymers [Ulr96].

Due to the increased demand for ultrapure materials and energy saving, the solvent-free melt crystallization technologies gained more importance in recent years. Most organic substances with melting points between - 50 and + 200 °C that does not decompose can be separated by melt crystallization. This technology is being already applied for purification of many different substances by industry e.g. xylene,

naphthalene, bisphenol, benzene-dichloride, mono chloroacetic acid, hexamethylene diamine, xylol and acrylic acid etc [Ulr96].

The purification of industrial product by melt crystallization can be carried out by a layer or suspension crystallization. In layer crystallization, a crystal layer is produced on a cold surface from the stable melt while in suspension crystallization a crystal suspension is produced in a simply stirred vessel containing a feed melt by cooling the entire melt. The separation of solid-liquid is very easy in layer crystallization mode because it requires the handling of liquid phases. Whereas in suspension crystallization, the solid-liquid separation is a little bit difficult as it requires additional equipment like filters and centrifuges which lead to a complex operation.

The layer melt crystallization technique has an advantage of the simplicity of an easy scale up over the other melt crystallization technique. It can easily be built up and modified at lab scale. It also provides the necessary preliminary data like crystal growth rate, maximum achievable purity and necessary temperature program required for the implementation of melt crystallization for the new products on an industrial scale.

Therefore, in this work applicability of layer melt crystallization for separation of complex feed streams of a multi-component product (two components and impurities) shall be evaluated. First, the purification of a complex feed stream by melt crystallization shall be measured by studying different optimization parameters like crystal growth rate, crystallization time and purity. Whereas in a second step, the desired composition of the final product shall be achieved by adding components resulting from the second stage of crystallization since the first crystallization gave only the desired purity, but did not give the right mixture of the two compounds of the desired product.

Hence, the aim of the above-mentioned task will be to increase the purity of the material to a level which is to date not achievable by distillation as well as to keep the ratio of isomers constant in a final product to maintain the product quality.

2. State of the art

2.1 Melt Crystallization

Crystallization is usually defined as a formation of solid state when a solution is supersaturated. Supersaturation is generally caused if solid-liquid equilibrium is disturbed by adding or evaporating the solvent, cooling of the complete system or by both. In a case of melt crystallization supersaturation is generated by cooling the melt, therefore, a term “supercooling” is used instead of supersaturation for melt crystallization [Hen10].

In crystallization processes, two terms are often used, “crystallization from solution and crystallization from the melt”. To precisely differentiate the mechanism of the solution and melt crystallization, Ulrich [Ulr03a] suggested a scientific definition. “Whenever the heat transfer is dominating a process of solid-liquid phase change, it should be called melt crystallization, while a mass transfer is a dominant process in solution crystallization”. Additional clarification may be obtained from the phase diagrams; the solubility diagram represents only a part of a phase diagram of melt equilibria and can be interrelated with each other as shown in Fig. 2.1.

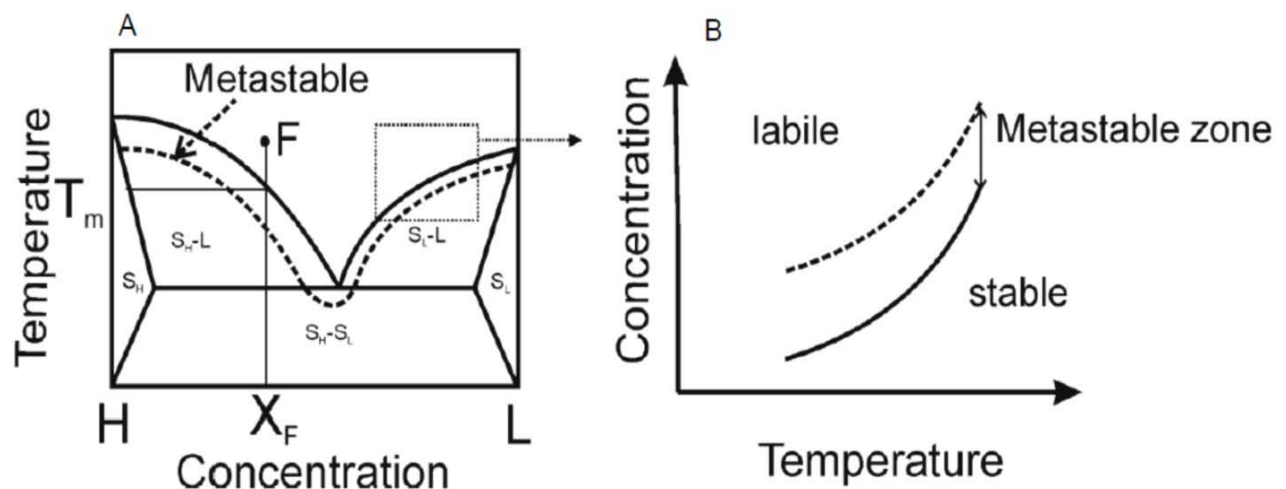


Fig. 2.1 Relationship between the solubility diagram and binary phase diagram [Cha10]

2.1.1 Solid-liquid equilibrium

The knowledge of solid-liquid equilibrium is very important in order to design a melt crystallization process as a product purification and separation step. The solid-liquid phase diagrams are graphical representation of the phase equilibria and are used to obtain a first indication of separation of components from the mixture by thermodynamic perspective. It also contains the information on the process condition with respect to purification, e.g. feed composition, process temperature under which A and B can be separated etc.

The complexity of the phase diagram increases with the number of components. The binary component systems are simple and are well documented, whereas the ternary phase diagrams are very complicated and are not often described in the literature. The data on the multi-component systems are almost never available. In practice, the multi-component systems are of great interest and are simply treated as a combination of simple binary systems. This simplification is only valid when each impurity behaves independently of the other in relation to the main component [Ark95a] [Jan94].

Binary solid-liquid phase diagrams are divided into two categories: **Eutectics** and **Solid solutions** which exhibit partial or complete solid solubility.

Matsuoka [Mat77] published an analysis of a large number of binary organic solid-liquid systems in 1977. According to this analysis, 86% of the binary organic mixtures belong to the category of eutectic systems. Out of which 54.3% exhibit simple eutectic behavior and hence allow the separation of pure crystals in a single step of purification. The remaining 14 % form a solid solution and require a multi-stage operation.

2.1.1.1 Eutectic phase diagram

The understanding of binary eutectic phase diagrams is very important for making preliminary estimations on melt crystallization's feasibility. The material can almost be purified (from the side which has usually very small solubility next to the pure compounds) in a single step of purification in melt crystallization if the system shows a

binary eutectic behavior. The generalized binary eutectic phase diagram is shown in Fig. 2.2.

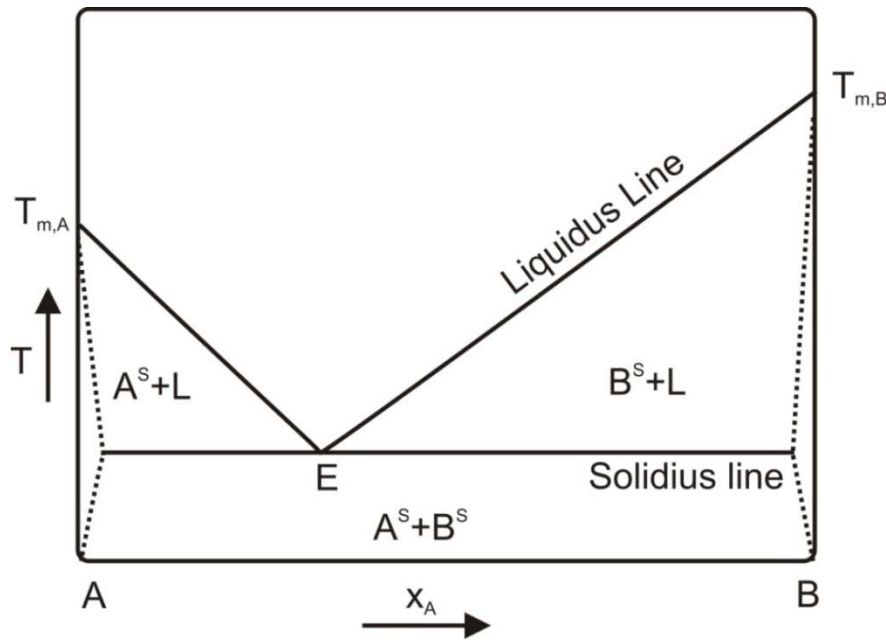


Fig. 2.2 Generalized binary eutectic phase diagram

The liquidus curves describe the equilibrium between the liquid mixture and pure solid at a given temperature. The theoretical shape of the liquidus curves of a component ‘i’ (where i = A, B) can be calculated by using the equilibrium condition when the chemical potential μ_i^L of the liquid in the mixture is equal to the chemical potential μ_i^S of the solid as given in Eq. 2.1.

$$\mu_i^L = \mu_i^S \quad \text{Eq. 2.1}$$

Under the assumption of an ideal mixture the chemical potential of the component ‘i’ can be written as a function of given temperature and the mole fraction x_i of the component ‘i’.

$$\mu_i^L = \mu_{i0}^L + RT \ln x_i \quad \text{Eq. 2.2}$$

μ_{i0}^L is the standard potential and R is the real gas constant.

Since, the change in the Gibbs free energy is zero at equilibrium; the temperature dependence of the mole fraction is x_i at equilibrium can be calculated by Schröder-van Laar Equation.

$$-\ln x_i^L = \frac{\Delta H_{m,i}}{R} \left[\frac{1}{T} - \frac{1}{T_{m,i}} \right] \quad \text{Eq. 2.3}$$

$T_{m,i}$ is the melting temperature of the component 'i' and $\Delta H_{m,i}$ is the molar heat of fusion.

The above equation is valid for the ideal mixtures and for the real mixtures, the activity coefficient is considered in the logarithmic term on the left side of Eq. 2.3 [Ark95a] [Sla95].

The dotted lines in Fig. 2.1 mark the areas of solid solution which occur due to the certain amount of miscibility in the solid phase. The width of this area in most cases is too small to be of interest. In a binary system, the separation of complete pure A or B is not possible. The impurity content can be extremely low but never be zero [Kön03].

The liquidus curves of the component A and B intersect at the eutectic point E. At this point, all the three phases (liquid mixture and the solid phases) co-exist. The eutectic point and its respective concentration limit the yield of a crystallization step. The maximum theoretical recovery of the component from any eutectic process can be calculated from the phase diagram by relating the concentrations as shown in Eq. 2.4.

$$R = \frac{x_F - x_{EP}}{x_F(1 - x_{EP})} \quad \text{Eq. 2.4}$$

where x_F and x_{EP} are the molar concentration of the main component at feed and eutectic point.

The solidus line separates the two-phase area of the solid phases from the two-phase area of the solid component (A or B) and the liquid phase.

2.1.2 Industrial crystallization techniques

The industrial separation and purification of the product by melt crystallization can be carried out by a suspension or layer crystallization mode. **Layer crystallization** is a well-known technology and is quite easy to operate. The driving force for the crystallization is generated by inserting a cold surface into the melt. Because of this temperature difference between the cold surface and the melt, the crystal layer begins to grow on the cooling surface. The high driving force results in a fast crystal growth rate so that impure melt is entrapped in the crystal layer. Consequently, the required purity is not attained in a single step and further purification steps (either more crystallization steps or sweating or/and washing steps) have to be performed. In the end, the residual melt is drained off and the crystal layer is melted.

In **suspension crystallization**, the crystals grow in the melt just below the melting point temperature and are surrounded by the melt. Therefore, the heat of fusion is removed through the melt and sub-cooling can only be moderate. As a result, crystals grow at low rates and a very pure product is obtained in a single step. After crystallization process, pure crystals must be separated from the contaminated residual melt. This requires the additional solid-liquid separation technique like filtration and centrifugation, which often leads to the complex operations [Ulr96].

For many chemical applications the applicability of the solid layer crystallization technique is increasing, especially, owing to the high environmental safety, easy scale-up and the possibility to connect all process steps in one apparatus. The problem of low purity at a high growth rate can be solved by using suitable post-crystallization step like sweating or washing.

2.1.3 Basics of solid layer crystallization

The initial step to start the crystal growth is nucleation during which small nuclei appear on the cooled surface and continue to increase to form the crystals with specific size. The nucleation is of two types homogeneous and heterogeneous nucleation. The most common way to start and maintain the crystallization in solid layer technique is

heterogeneous nucleation, which is produced by using the roughness on the cold surface [Ulr96].

In the layer growth, the driving force is the temperature gradient between the equilibrium melt temperature in front of the layer and the feed temperature. The growth of the crystal layer takes place directly on the cooled solid surface. The schematic concentration and temperature profiles for layer growth under stable condition are shown in Fig. 2.3a. The heat of crystallization is directly removed from the process through the crystal layer and the cooled surface. The formation of the pure crystal layers is possible if the solid phase is in equilibrium with the liquid phase and growth rate is small.

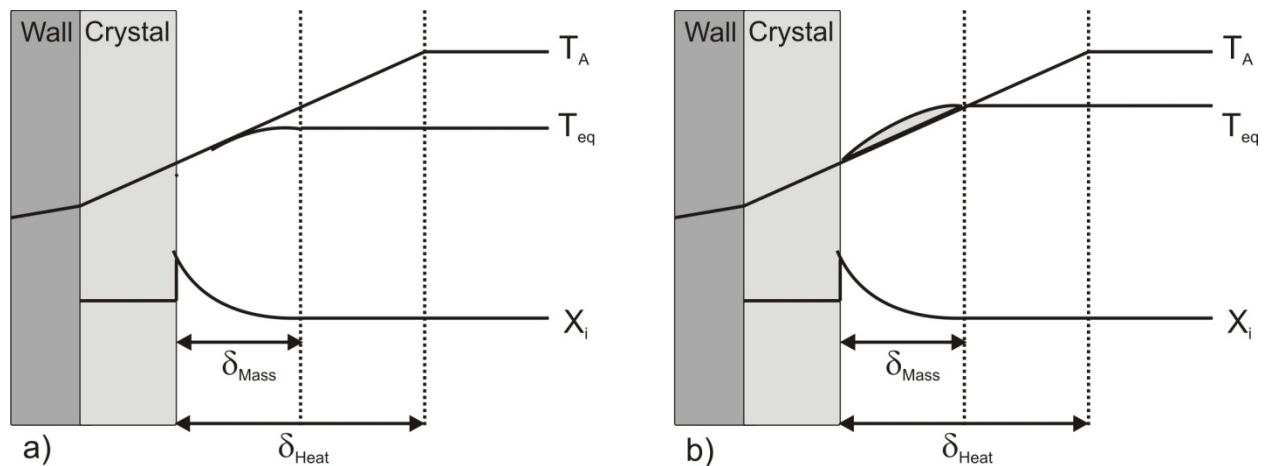


Fig. 2.3 Profiles of layer growth: a) stable conditions; b) unstable conditions [Hen10]

On the other hand, the fast crystal growth rate leads to high supercooling from crystal layer toward the bulk, which leads to the incorporation of the impurities (solid material or and liquid inclusions) in the crystal layer in front of the melt. Moreover, this impurity gradient in the crystal boundary layer lowers the equilibrium temperature (T_{eq}) and therefore the supercooling increases the rough growth (dendrite outgrowth) on the crystal surface. This behavior favors an unstable growth and is known as constitutional supercooling [Hen10]. This phenomenon usually occurs on the industrial scale due to fast growth rate and is responsible for the low purity in a single step of crystallization. The temperature and concentration profile of the boundary layer at unstable conditions are shown in Fig.2.3b.

2.2 Purification mechanism of industrial layer melt crystallization

In the solid layer crystallization, the crystal layer begins to grow immediately on a cooled surface when cooling plates are immersed in the melt. The direction of the crystal growth is perpendicular to the surface into the bulk of the mother liquor while the heat of fusion is removed through the crystalline layer and cooled wall. The temperature of the plates (cooling or heating) used for crystallization is controlled by an internal circulation of a suitable heat transfer medium. The schematic diagram of the static layer crystallization showing the different phases occurring during a single crystallization step is shown in Fig. 2.4.

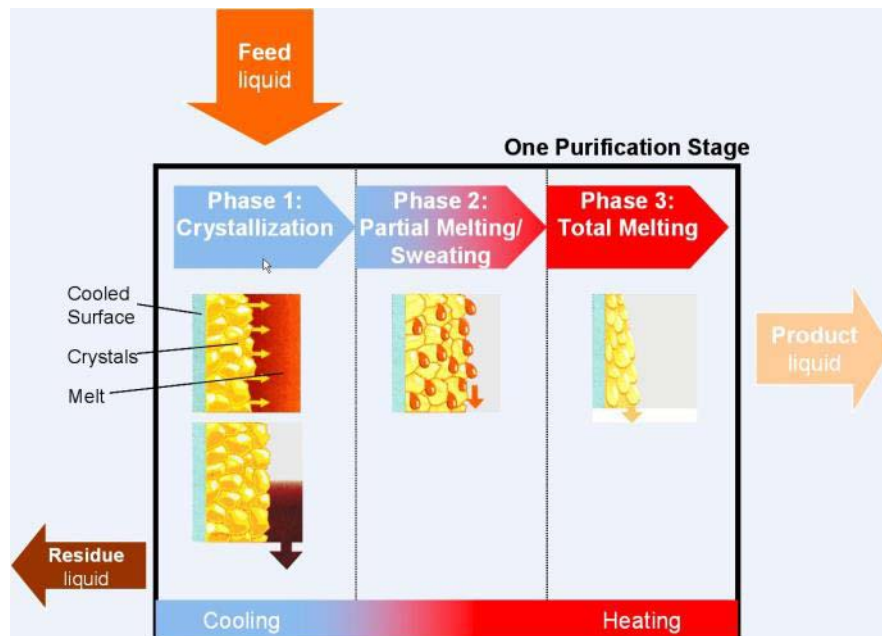


Fig. 2.4 Different crystallization stages [Ste03]

Usually, the single batch of layer crystallization is divided into the three phases of operation.

2.2.1 Crystallization

In the first step, already tempered (rough) cooling surfaces at a set temperature are immersed into the crystallizer containing melt. The temperature of the cooled surface is kept below the freezing point of the melt by a cooling medium. This immediately leads to the nucleation on the cooling surface and then the crystal layer begins to grow for a

certain period of time. After, the desired fraction has been crystallized on the cooled surface, the remaining melt is drained off from the crystallizer. The crystal layer remains adhered to the plates and is used for the further purification step like sweating.

2.2.2 Sweating (partial melting)

After crystallization, the crystal layer is further purified by a post-crystallization step like sweating (partial melting). In layer crystallization, sweating is applied to remove the impurities attached to the crystal surface. Sweating needs a much shorter retention time and is, therefore, faster as compared to the crystallization process. The sweating is done by raising the temperature of the layer close to its melting point. A partial melting of the layer induced by a rise in temperature leads to a lower viscosity of the inclusions and a high porosity of the crystal layer, which cause the impurities and liquid inclusions to drain out under the influence of gravity as a sweating liquid [Bei13] [Kim02]. Consequently, the trapped and adherent melt which contains impurities is drained off from the crystal layer as a sweating liquid.

The other key advantages of partial melting is that it also rinses the crystallizer free of impure melt, preventing the back mixing and contamination of the final purified product [Ste03].

2.2.3 Total melting

At the end, the product is subsequently recovered by totally melting the purified crystal layer to its melting temperature from the cooling surface and is drained to provide the pure product. There is no extra energy needed for the phase transformation to remove the layer from the cooling surface, as the crystal layer is already partially melted due to the sweating. Hence, the certain amount of the energy can be saved.

The other advantage of this technique is that it does not require any other unit operation or mechanical means to remove the purified product from the liquid.

The operating temperature conditions during all three steps involved in crystallization process is schematically plotted with respect to crystallization time and shown in Fig. 2.5.

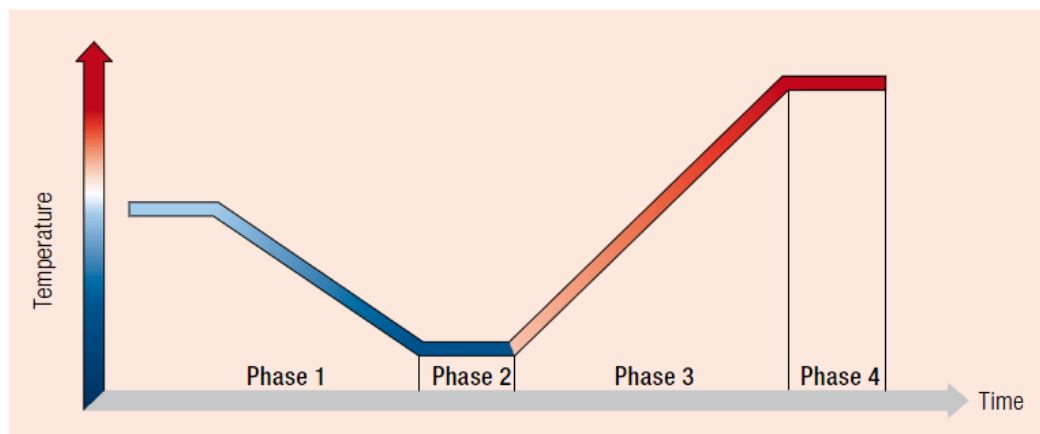


Fig. 2.5 Temperature profile during the static crystallization [Ste03]

2.3 Industrial problems

The last few decades are driven by strict governmental policies towards the chemicals disposal and emissions. Therefore, the chemical industries are looking for new innovative manufacturing processes and separation technologies to overcome all these problems. Therefore, the industry is developing and implementing the new separation technologies which can minimize the emission of solvents and reduce operator exposure to the chemicals, which are much needed in today's chemical industries.

As the industry concentrates its efforts more on the environmental and health aspects of chemical manufacturing, an example of currently available technology is melt crystallization. It can offer a unique potential for separation of the high-purity applications in addition to environmental and health benefits. Melt crystallization does not need any additional substances like solvents, e.g. in extraction. Therefore, there are no further impurities getting into the substance to be purified and no chemicals (solvents) have to be regenerated. As all the products are separated on the basis of the melting point, consequently, there is no existence of a vapor phase. This results in a better control of leakages and emissions of toxic compounds in the environment. The totally closed equipment leads to the high environmental safety.

Besides these environmental problems, the chemical industry is very much concerned with the separation and purification of chemical compounds due to the increase in demand for more pure products. Impurities generally represent wasted product and

cause undesirable variations in the final product quality. Specific impurities can damage catalysts and can lead to failure of downstream processes. A maximum purity of the products can be achieved within a single separation step by the melt crystallization if a system to be separated is the eutectic one. This high selectivity is not possible by any other separation technique.

Distillation is still being used as the industry standard for the separation of organic materials for most chemical separations. It has developed into a reliable unit operation that is widely used when conditions allow the stage-wise contacting of multi-component liquid and vapor. Melt crystallization is an economical and effective alternative. It is typically used in purification application where distillation becomes impossible or at least difficult, e.g. many materials which have close boiling points like different isomers, azeotropic mixtures and heat sensitive materials which are difficult to be purified by conventional technologies like distillation.

The other major advantage of melt crystallization as a separation technology is less energy required for phase transformation (liquid/solid) compared to other techniques like distillation (liquid/vapor). The heat of transformation in melt crystallization is 2 to 5 times lower than distillation. This is due to the relatively low of temperatures (melting point) and the much smaller latent heat is required for a phase change.

In recent years, the chemical process industries have become more aware of the inherent advantages afforded by melt crystallization. This technology can also be used as an alternative to the conventional separation processes like distillation, and absorption, particularly when the high purity of the product is needed. This process is not only applicable for new grass root plants but is also appropriate to upgrade the capacity and purity (quality of the product) of existing processes. Small changes to existing units can significantly increase the product purity requirement of an existing process.

The detailed information on the background and fundamentals about the melt crystallization can be found in Arkenbout [Ark95], Jansens and van Rosmalen [Jan94],

Ulrich and Bierwirth [Ulr96], Ulrich and Bülau [Ulr02], Ulrich [Ulr03], Ulrich and Nordhoff [Ulr11], Ulrich and Stelzer [Ulr13], Verdoes [Ver97].

3. Objectives of the work

In practice, multi-component systems are of great interest, especially, when technically dealing with the multi-component mixtures or complex feed streams of a product, e.g. edible oils, fats and waxes, etc. In most cases, it is difficult to separate these multi-component products and requires an appropriate procedure for the separation and purification. The treatment of the complex feed streams of products is usually simplified by considering these systems as a combination of separate binary systems. This simplification is, however, only valid if the higher order interactions between the components of the system do not exist and when each impurity behaves independently of the other in its relationship to the main component [Ark95a] [Jan94]. Melt crystallization is known to work often quite well if the mixtures are eutectic in nature.

Therefore, in this work, the feasibility for an implementation of layer melt crystallization for the separation of the multi-component complex feed streams of products is evaluated. The complex mixture of a feed stream is taken as a case study. The product is an important technical product. It is a mixture of different components (different isomers and impurities), some of which show eutectic behavior while others do not and also contain some impurities which decrease the overall purity of the product. Furthermore, a restriction on the composition of the main components in the end product is given.

To achieve the purification, a new approach as discussed above will be adopted for the separation of the multi-component products in order to keep the right ratio of the isomers as well as to increase the overall purity of the final product. During the experiments, one material will be taken as a pure material and will be separated first while others will be taken as an impurity (as done so far, in order to have a binary component phase diagram). This “new” impurity shall be treated afterward again by a melt crystallization process just like a binary component system. This procedure shall be repeated again and again until the two isomers will be separated from each other. At the end, all separated streams with a high purity shall be mixed together to get the right (the wanted) mixture of isomers.

Hence, the main task of the thesis is to investigate the technical feasibility of the multi-component complex feed streams of product separation by layer melt crystallization at the purity level of the material which is to date not achievable by distillation as well as to keep the ratio of isomers constant in a final product to maintain the product quality. As a precondition, it also requires the basic knowledge of thermodynamics (solid-liquid equilibrium) and kinetics by studying the effect of growth rates and crystal morphology at different conditions. Therefore, the sub-objectives of this thesis are:

- Investigations of solid-liquid equilibrium between different components to check whether this system can be separated by melt crystallization.
- To investigate the effect of different process condition on crystal growth rate and crystal morphology. As the knowledge of crystal growth rate is very important for the design of crystallizer.
- Elaboration of improvement in different process condition of crystallization to maximize the yield of the process.
- Calculation of the phase change energies to calculate the energy demand of the process.
- To implement this method for the separation of another isomer (3-isomer) this is also an important component of the main component of the product.

4. Materials and Methods

This chapter gives a detail description of the materials used in this work. Experimental methods and protocols adopted for the separation and purification of the product. In the end, different analysis strategies and techniques for prediction of results are discussed also in detail.

4.1 Materials

4.1.1 Raw Product 'A'

The industrial raw product with multi-components was provided by an industry for a study. It is a mixed product of two major isomers '3-isomer' and '5-isomer' with some impurities 'Imp'. The ratio of the 3-isomer is 64% in the product 'A' while the ratio of 5-isomer 36%. The overall purity of the product 'A' (3-isomer and 5-isomer) is 95% and it contains 5% of impurities which are the traces of untreated material or side products of the reaction.

This product is present in a solid state with yellowish brown in color. It has a melting point in a range of 94.5 - 121.9 °C and boiling point is 270.7 °C. The composition of the product 'A' is given in Table 4.1.

Tab. 4.1 Composition of Product 'A'

Component [%]	Impurities [%]
Product 'A' (95%) (3-isomer and 5-isomer)	Acetamide and 3 (5) methyl pyrazole derivatives, Water and formaldehyde (5%)

4.1.2 3-Isomer

The other important material is 3-isomer which is also a major constituent of the main raw product and is also provided by the industry. It is a solid material with light yellow color. It has a melting point in the range of 102-104 °C and boiling point is 250 °C. It has a purity of 83% and contains 14% of 5-isomer as an impurity and 3% of other impurities

like 3-Methylpyrazol, Acetamide and water. The detail about the composition of 3-isomer is given in Table 4.2.

Tab. 4.2 Composition of 3-isomer

Component [%]	Impurities [%]
3-isomer (83%)	5-Isomer (14%),
	3-Methylpyrazole, Acetamide and water (3%)

4.1.3 5-isomer

It is a white solid in the form a fine powder. It has a melting point in the range of 154 to 158 °C. It has a purity of about 93% and contains 7% of 3-isomer in it.

These two isomers are separated from the main technical product by using the different water solubility of these isomers.

4.1.4 Methanol

Methanol is the simplest alcohol with chemical formula CH_3OH . It is a light, volatile, colorless and flammable liquid. High performance liquid chromatography (HPLC) grade methanol with 99.9% purity from VWR International GmbH was used for HPLC analysis. It was used for two purposes, first as a solvent for the preparation of samples for HPLC analysis after crystallization. Secondly, it was used as a mobile phase in water/methanol low-pressure gradient HPLC for the analysis of the ratio of the two isomers (i.e. 3 and 5-isomer) in the product.

4.1.5 Acetonitrile

It is a colorless liquid with a chemical formula CH_3CN . It is a medium-polarity solvent and is immiscible with water. HPLC grade acetonitrile with 99.9% purity from Carl Roth GmbH & Co.KG was used in this work. It is used in as a mobile phase in water/acetonitrile low-pressure gradient HPLC for the analysis of purity of the main product and 3-isomer.

4.1.6 Benzoic acid

It is a colorless crystalline solid with chemical formula $C_7H_6O_2$. It has melting point at 122.41 °C and a boiling point at 249 °C. Benzoic acid with purity up to 99.9 % from Merck KGaA was used as a reference material for the calculation of heat of vaporization.

The details of the all chemical used in this work with their analytical use, supplier and specification are given in Table 4.3.

Tab. 4.3 Summary of chemicals used in this work

Chemical	Provider	Use	Purity [%]
Methanol	VWR International GmbH	HPLC (mobile phase) for measuring the ratio of 3&5-Isomer in a product	99.9
Acetonitrile	Carl Roth GmbH & Co.KG	HPLC (mobile phase) for measuring the purity of the product	99.9
Benzoic acid	Merck KGaA	Used as a reference material in heat of fusion and vaporization calculation	99.9

4.2 Experimental methods

4.2.1 Solid-Liquid equilibrium

In order to separate a mixture of any organic material by melt crystallization, the knowledge of the solid-liquid equilibrium (SLE) is very important. Its can help to check whether separation is possible or not by crystallization and also give an estimation of the process operating conditions [San94]. For the construction of solid-liquid phase diagram, measurements were carried out in a Netzsch DSC from Erich Netzsch GmbH & Co. Holding KG for a mixture of different concentration of two pure isomers.

4.2.1.1 Differential scanning calorimetry (DSC)

Differential scanning calorimetry is an established and widely used analytical technique in different fields of research. In crystallization, it is used to estimate the solid-liquid equilibrium focused on the melting point phase diagram which describes the melting

behavior of the two components in the system [Moh02]. Differential Scanning Calorimetry (DSC) measures the temperatures and heat flows related to transitions in materials as a function of time and temperature in a controlled atmosphere. These measurements provide quantitative and qualitative information on physical and chemical changes that are involved in an endothermic or exothermic process, or changes in heat capacity [Gab08].

a) Sample preparation

To obtain a uniform mixture of material, 100 mg of the mixture containing both pure isomers from a raw product in different amounts was taken and grinded in a mortar. After that, this mixture was melted in an oven to its melting point and it was stored at the cool place for recrystallization. This recrystallized mixture was grinded again and was used for the DSC analysis [San94], [Shi93]. This was done to ensure that the sample mixtures were mixed uniformly to eliminate any possible sources of analytical errors. The same procedure was repeated for making the other mixtures by using the different ratios of pure isomers.

b) Analysis of samples

After preparing the sample, 7 ± 0.03 mg of the sample was taken in aluminum crucibles every time for DSC analysis. The crucible was sealed with an Al lid and a small hole was punched in the lid. DSC scans of each mixture were performed at a low heating rate of 2 K/min in the temperature range of 20 - 200 °C. The DSC cell was purged with a stream of dry nitrogen at a rate of 30 mL/min. Experiments were performed three times to check the reproducibility of the measurements and mean values were calculated. After each measurement, the enthalpies of the fusion of the pure components and solid-liquid equilibrium of the mixture were measured by calculating the onset and peak temperatures of DSC isotherms. Then these values were plotted together to construct the solidus and liquidus curves of a phase diagram [Tak02].

4.2.2 Experimental set up for crystallization

Crystallization was carried out in a laboratory-scale cold finger apparatus (static solid layer melt crystallizer) [Gla03] [Ulr13]. The schematic diagram of this lab scale cold

finger apparatus with its essential parts is shown in a Fig. 4.1. It consists of a double walled glass beaker with an inner diameter of 40 mm and depth of 85 mm to melt the feed material to its melting point, cylindrical tube steel cold finger with an outer diameter of 20 mm for crystallization. The temperature of the double walled glass beaker containing the feed melt and steel cold finger was controlled by the two different thermostats, respectively.

The cold finger is an internally cooled tube by circulating a coolant through it for crystallization. The driving force in solid layer crystallization is a temperature difference between the melt and surface of the cold finger, which can determine the growth rate and consequently maximum achievable purity. Therefore, important parameters like growth rate, achievable purity and optimal temperature program for the design of an industrial scale crystallizer can easily be investigated by this cold finger experiments [Ulr13].

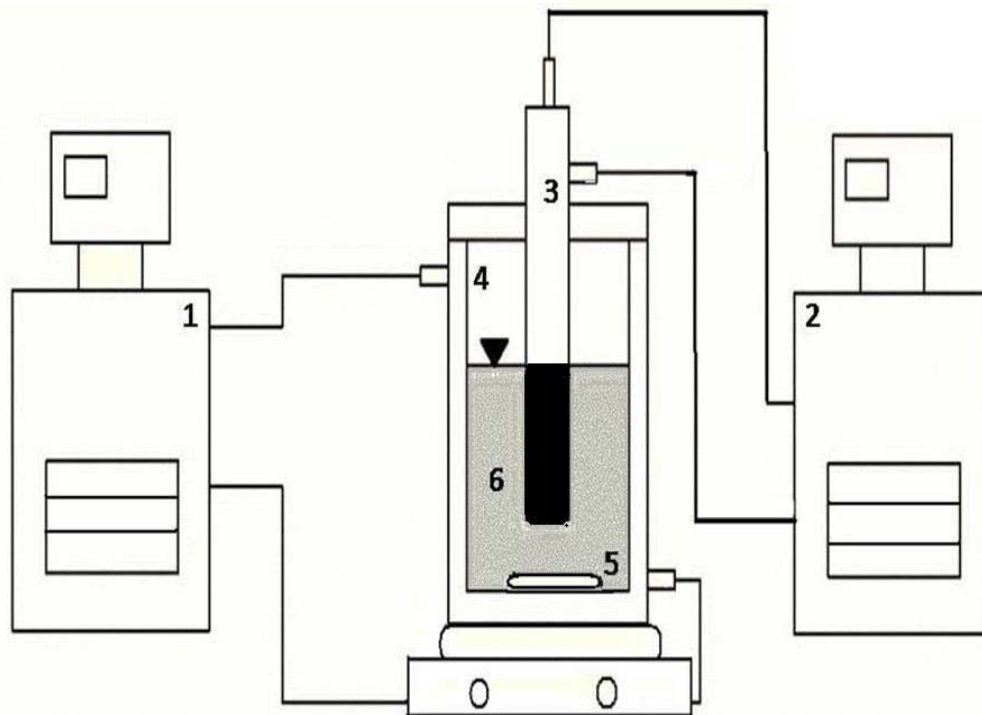


Fig. 4.1 Sketch of experimental setup: (1,2) Thermostats; (3) Cold finger; (4) Double wall beaker; (5) Magnetic stirrer; (6) Melt

4.2.2.1 Procedure for experiment

First, 50 g of the material was taken in a double walled beaker. It was heated up to its melting point, i.e., 130 °C, slightly above its melting point so that all the material will melt and meanwhile the vessel was covered with a lid. Then an already tempered cold finger at different temperature levels was inserted into the crystallizer from the top and was fixed with a stopper, which simultaneously closed the vessel as well. This immediately leads to the nucleation on the surface of the cold finger and after that, the crystal layer begins to grow on the surface of the cold finger for a certain period of time as shown in Fig. 4.2.

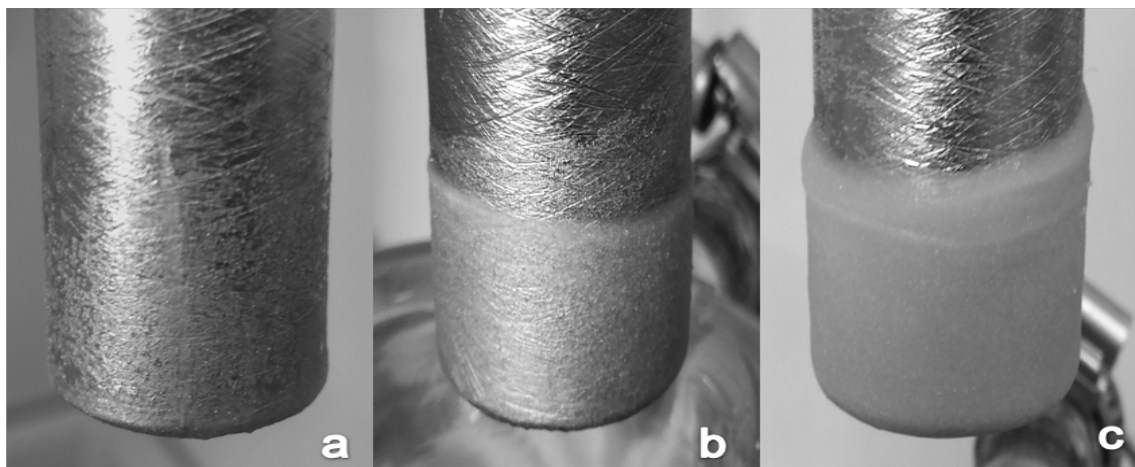


Fig. 4.2 Mechanism of crystal growth on a steel cold finger: (a) Nucleation; (b) Crystal growth; (c) Final crystal layer

The temperature of the cold finger was kept constant during crystallization by a second thermostat. It was repeatedly crystallized from the initial melt at different times to check the effect of layer thickness and purity. After the crystallization was completed, the cold finger was removed from the remaining melt. At the end, the layer thickness and growth rates were measured for each experiment. Samples were taken from different positions on the layer for purity and the ratio of isomers analysis by HPLC. The adhering residual melt on the cold finger was molten and dropped back into the crystallizer vessel.

The experiments were carried in four different batches to separate the two isomers in the product 'A' by treating the residual melt. In the end, the product from all different

batches with different ratios of isomers and purity were mixed together to maintain the product specification with maximum possible purity.

4.2.2.2 Sweating

For further purification of the crystal layer, post-crystallization step like sweating was carried out after each experiment for different times by placing the cold finger in another beaker. Then drain out of the melt during sweating was collected in that beaker. The temperature of the cold finger was increased up to 110 °C, 10 °C below to the melting point of the crystal layer. The temperature of the cold finger was kept constant and the small amount of the samples was taken after each 15 min. These samples were analyzed for the purity and composition (ratio of two isomers) by HPLC.

4.2.2.3 High Performance Liquid Chromatography

It is generally used for the separation of the different compounds from the mixture of components. It is done by injecting a small amount of sample into a moving stream of a solvent called mobile phase. Then, this mixture is passed through a packed column, which is packed with particles of stationary phase. The separation of a mixture into its components depends on different degrees of retention of each component between the mobile phase and the stationary phase. Since the different compounds have different mobilities because of their densities and viscosities in a mobile phase, they exit column at different times. This time is known as a retention time. Each component has a different spectrum and retention time at a specific wavelength which is detected by a detector. This information is converted into an electrical signal [Bro97] [Sko98] and is recorded in a computer. Now different computer software provided by HPLC manufacturers are used for the analysis and recording of the data. The schematic diagram of an HPLC system is shown in Fig. 4.3.

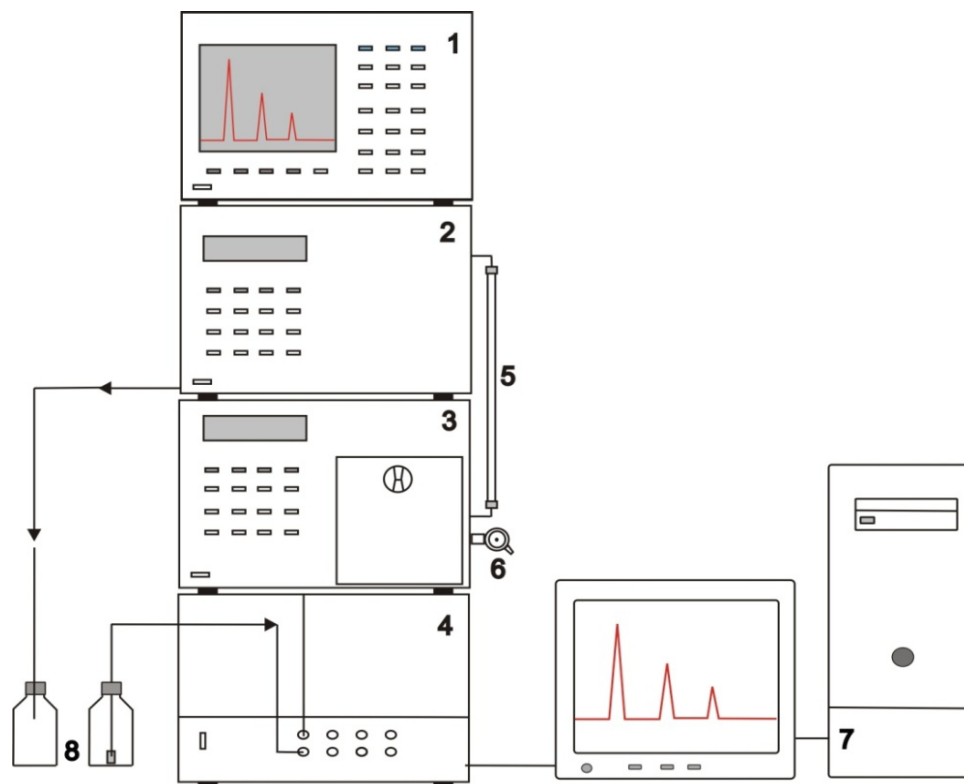


Fig. 4.3 Basic setup of HPLC by Shimadzu: 1) Controller; 2) UV/Vis detector; 3) Pump; 4) Degasser; 5) Column; 6) Injection valve; 7) Computer; 8) Solvent

4.2.2.3.1 HPLC analysis

For the analysis and quantification of samples, a special method and technique is required to get the suitable peaks by the HPLC. For this reason, two different methods were used for the HPLC analysis. The first method was used for measuring the purity of the samples by HPLC (method 1) and the second method was used for measuring the ratio of two isomers in the product by HPLC (method 2). Both these methods were provided by our industrial partner. Both HPLCs used are from the Shimadzu HPLC system and detail of the all major components of both HPLCs is given in Tab 4.4.

Tab. 4.4 Detail of components of Shimadzu HPLC system

Component	Method 1 (for purity)	Method 2 (for isomers ratio)
System controller	Shimadzu CBM-10A	Shimadzu SCL-10A VP
UV/Vis detector	Shimadzu SPD-10A	Shimadzu SPD-10A.VP
Pump control	Shimadzu LC-10AD VP	Shimadzu LC-10AT VP
Low-pressure gradient unit	Shimadzu FCV-10AL VP	-
Degasser	Shimadzu DGU-14A	Shimadzu DGU-3A
Injection valve	Rheodyne, Injection volume 20 μ L	Rheodyne, Injection volume 20 μ L
Software	Shimadzu Class LC10	Shimadzu Class VP
Column	Nucleosil® 50-5 C8, 5 μ m packing: Dimension 250 mm length and 4mm inner diameter	Eurosphere 100 C18, 5 μ m: Dimension 250 mm length and 4mm inner diameter
Eluent	Water/Acetonitrile (80/20 v/v %)	Water/Methanol (80/20 v/v%)
Wavelength	205 nm	218 nm

To check the purity of layer after crystallization method 1 was used. Each sample was prepared by taking a 0.1 mg of the material from the crystal layer and then dissolving it in a 100 μ L of methanol in a small bottle. After that, the solution was filtered so that there will be no solid particles left in this solution. Then, 20 μ L of the solution was injected into the HPLC with the help of syringe for the analysis. For stationary phase prepacked column from Macherey Nagel (Nucleosil ® 50-5 C8, 5 μ m packing) having a length of 250 mm and 4 mm inner diameter was used. The mobile phase consisting of water and acetonitrile in a ratio of 80/20 v/v % with low-pressure gradient mode was pumped at the flow rate of 1mL/min for 1 h.

In HPLC this gradient elution is normally used to adjust the strength of the mobile phase for better results. It can also be used to produce high peak heights in a shorter

operation cycle [Shr12]. The different peaks were detected at the wavelength of 205 nm by their characteristic of retention times and spectra. Shimadzu Class LC10 software was used for analyzing the data.

Similarly, the ratio of the isomers in the product 'A' is measured by using a method 2. In this method, the ratio of the two isomers was detected by using a mobile phase with water and methanol in a ratio of 80/20 v/v% in low-pressure gradient HPLC for 30 minutes. The prepacked column from Knauer with packing (eurosphere 100 C18, 5 μ m), having a length of 250 mm and an inner diameter of 4 mm was used. The peaks of the isomers were detected at the wavelength of 218 nm by a UV/Vis detector. Shimadzu Class VP software was used to analyze the different peaks and data.

4.2.3 Crystal morphology

Measurement of crystal morphology is of great interest in research to understand the crystal growth mechanism and its habit to grow. Widely used techniques to measure the crystal morphology are microscopic and digital video imaging [Sin12]. In this work, the growth and morphology were recorded with the help of a Keyence digital microscope (VHX500F) connected to an advanced (high resolution) CCD digital camera for recording and taking the picture of crystals after fixed intervals. The lens (VH-Z100R) with a magnification power of 100×1000 was attached to the microscope for the magnification of the images of the crystals. The schematic diagram of the setup is shown in Fig. 4.4.

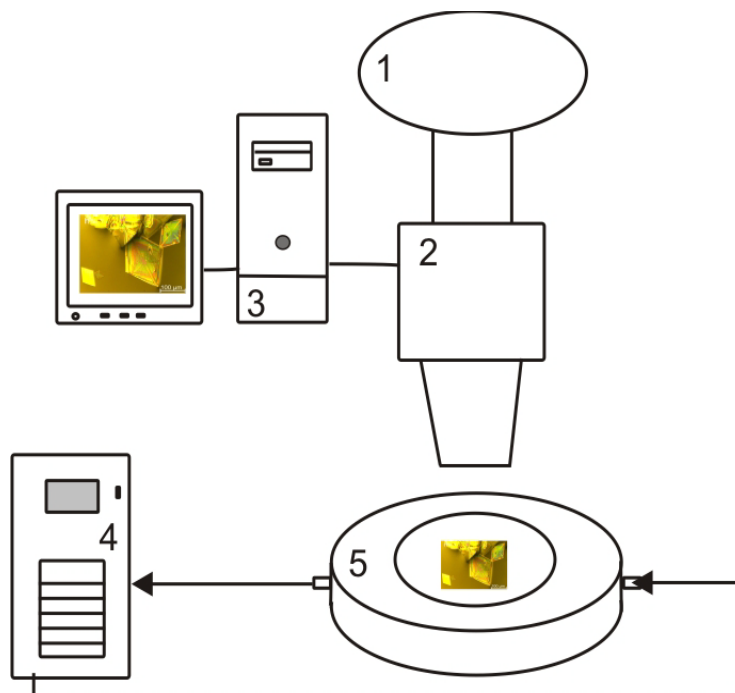


Fig. 4.4 Setup for microscope 1) Camera; 2) Microscope; 3) Computer; 4) Thermostat; 5) Microscopic cell

4.2.3.1 Analytical method

The experiments were carried out in two parts, first sample preparation for the analysis and then analyzing a sample under a microscope to get some picture of single crystals.

First, 10 mg of the sample was taken on the small glass slab and was molten up to its melting point by the use of a Kofler heating bench. It is used to find out the melting point of the material manually as shown in Fig 4.5.



Fig. 4.5 Kofler heating bench

After melting the material, this glass slab was put under the microscope on top of a microscopic cell. This microscopic cell was attached to a thermostat to control the

temperature of a cell for crystal growth. The crystals were grown from the pure melt under an optical microscope. These crystals were observed while growing in the melt and were photographed after a fixed interval of time for the analysis [Nie95].

4.2.4 Method for calculating heat of fusion and vaporization

As these products are in the preliminary stages of development and are still not available in the market. A very important thermal data for energy balance calculation are not available in the literature. It is important to calculate the values like a heat of fusion and vaporization. So that phase change energy values can be measured during crystallization (liquid-solid) and distillation (liquid-gas). Then these values were compared with each other, to check the feasibility of the overall process. This was performed by using a simultaneous TGA-DSC instrument.

The experiments were carried out in a Netzsch STA 409 from Enrich Netzsch GmbH & Co. The mass loss of the sample was measured by a TGA signal while melting and evaporating peaks were measured by DSC simultaneously during the measurement. These values calculated from TGA and DSC were co-related to calculate the heat of fusion and vaporization [Sau09].

For analysis, 10 mg of the pure samples were taken in an aluminium crucible. The scans for TGA-DSC were run 30 °C above the boiling point of the material, at the heating rate of 5 K/min and Helium was used as a purged gas. All measurements were repeated for three times to check the reproducibility and mean values were used for the calculation.

The summary of all analytical techniques used for the analysis of the results with their specification and limitations is shown in Tab. 4.5.

Tab. 4.5 Summary of all Analytical techniques

Sr. No.	Analytic technique	Supplier	Limitations
1	DSC	Erich Netzsch GmbH & Co. Holding KG	Operating temperature range from - 30 to 350 °C
2	TGA-DSC	Netzsch STA 409 from Erich Netzsch GmbH & Co.	Operating temperature range from 20 to 1700 °C
3	HPLC	Shimadzu HPLC system	Flow range: 0.001-5 mL/min at 10 - 400 Kgf/cm ² Wavelength range: 190 ~ 600 nm
4	Microscope	Keyence digital microscope (VHX500F)	With lens VH-Z100R max magnification power is 100 × 1000

5. Results

In this chapter the outcome of all the results obtained from different experiments for the purification and separation of the 'Raw Product 'A'' and 3-isomer are presented in detail. At first results for the solid-liquid equilibrium are presented to check the feasibility of separation by melt crystallization. Then, a simple laboratory scale melt crystallization setup is used for the separations of the different products. The separated components are analyzed with the HPLC by using the respective solvents. After that, crystal growth rates and the morphologies are studied by growing the crystals under a microscope. In the end, the calculation of phase change energies is tried to have a base for an energy evaluation of the whole process.

5.1 Case study I 'Raw Product 'A''

5.1.1 Solid-liquid equilibrium

To establish the crystallization process for the materials under consideration, it is very important to know the solubilities of these compounds to be crystallized. Therefore, the Schröder-van-Laar equation is used for this purpose and it applies to an ideal binary component system. In the first stage, the DSC measurements are performed for the pure product 'A' and 5-isomer to estimate the melting points (MP) and the heat of fusion (ΔH_f) of these components, which are contained in the raw product. The obtained thermograms of product 'A' and 5-isomer is shown in first and last isotherm in Fig. 5.1. The respective melting point and heat of fusion data are used to calculate the values of liquidus lines by computing these values in Eq. 5.1 and the calculated results are plotted in Fig. 5.2. The black line in Fig. 5.2 shows the results calculated by the Schröder-van Laar equation:

$$\ln(x_a) = -\frac{\Delta H_f}{R} \left[\frac{1}{T_m} - \frac{1}{T} \right] \quad \text{Eq. 5.1}$$

After that to validate the results obtained from Eq. 5.1, the solid-liquid equilibrium between product 'A' and 5-isomer was constructed experimentally by using a DSC. It is measured by taking a 7 mg of samples with different compositions of product 'A' and

5-isomer. Only one peak is observed for the pure components while two melting peaks are observed in all other cases for the binary mixture at each composition as it is to be seen in Fig. 5.1. On the composition of 10% of 5-isomer a very small second peak appears also in the isotherm, but due to the bad resolution, this peak is not clear in the isotherm. With the change in the ratio of the isomers, the magnitudes of the melting peaks also changed. The second peak grows in size with the increase in the amount of 5-isomer and moves to the right closer to the melting point of the pure 5-isomer. At the same time, the size of the first peak decreases and it is taken as the eutectic peak. All the thermograms measured by DSC for different ratios of the isomers are shown in Fig. 5.1.

The first peak with a lower temperature at close range corresponds to the melting of a eutectic mixture and is used to construct the solidus line while the second peak with the higher temperature is a characteristic of the liquidus equilibrium curve or melting point of major component [Cam10].

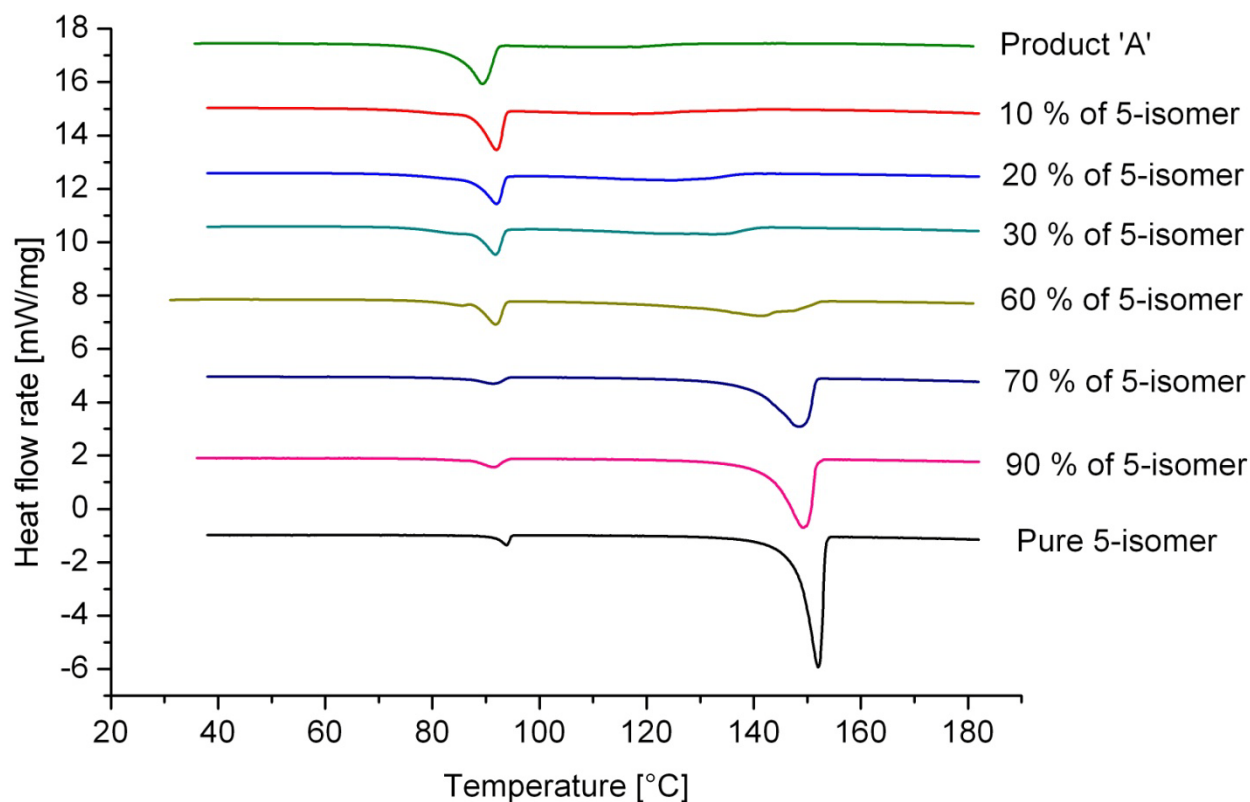


Fig. 5.1 DSC curves of product 'A' and 5-isomer

The onset temperatures of the peaks were taken as a melting temperature and the area under the curve was measured as a heat of fusion of these components. All these values were interpolated with each other to get the phase diagram of the binary system between product 'A' and 5-isomer. The liquidus lines of the system intersect at the value of 0.18 wt.% of 5-isomer and gave the eutectic point. These results clearly show that this system is a simple binary eutectic system with the eutectic point at a composition of 0.18 ± 0.02 wt.% and the eutectic temperature at 365 ± 3 K (91.85 °C). The theoretical yield calculated by the phase diagram is about 78%. In Fig. 5.2 the red points represents the curve measured experimentally by DSC while black lines represent a curve calculated by the Schröder-van-Laar equation.

Finally, the calculated and experimental values are compared with each other and they are found to be in good agreement with a standard deviation of approximately 5%.

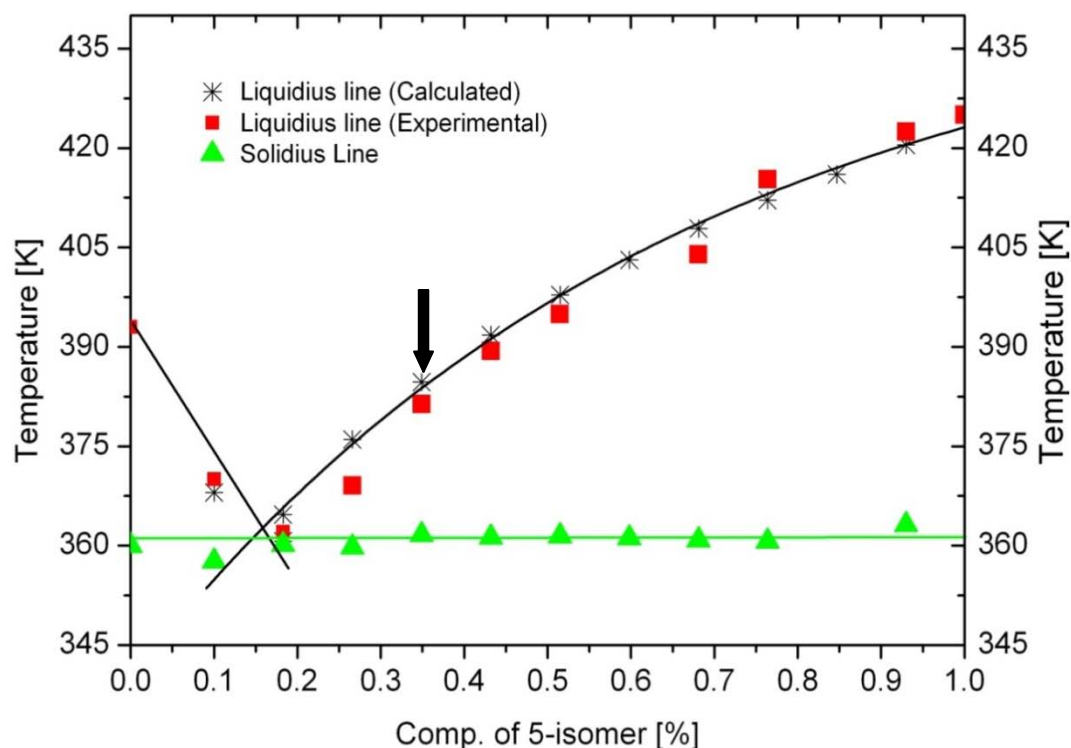


Fig. 5.2 Binary eutectic phase diagram between product 'A' and 5-isomer [Ahm15] [Ahm16]

As discussed in Chapter 4.1.1, the initial concentration of the product 'A' is 64% of the 3-isomer and 36% of the 5-isomer as shown by a black arrow in Fig. 5.2. This

concentration lies on the right side of the phase diagram where maximum amount of the 5-isomer is present. Therefore, when the temperature of the melt is decreased by inserting a cold finger, the 5-isomer began to crystallize along the liquidus curve of the 5-isomer as compared to the 3-isomer till the eutectic point is reached.

5.1.2 Average layer thickness at different temperatures as a function of crystallization time

In this section, the effect of the crystallization time on the crystal layer thickness is studied at different temperatures of the cold finger by using a lab scale layer melt crystallizer as shown in Fig. 4.1. All experiments are carried out three times and average values are used in these measurements. The cold finger was inserted into the melt at different temperatures or heating rates. The crystal layer began to grow on the surface of the cold finger immediately. The thickness and height of the layer were measured by vernier caliper from different points and mean values are used for the calculations.

The crystal layer grows rapidly in the beginning due to the high degree of supersaturation (ΔT). After 2.5 h the layer thickness reaches a maximum value and it slows down after reaching the equilibrium because of the increase in the thermal resistance between the crystal layer and the cold surface. This can be seen in Fig. 5.3. The layer thickness for the temperature of the cold finger at 65 °C and 70 °C are almost at the same value as shown in Fig. 5.3 due to the low-temperature difference (ΔT) between the melt and the surface of the cold finger. At smaller temperature differences (ΔT) the cooling rates are also low; the layer grows slowly and needs a longer period of time to grow.

It means when the temperature difference between the melt and cold finger (ΔT) is high, the degree of supersaturation is also high and layer thickness increases rapidly. On the other hand, at low cooling rates the layer grows slowly and it needs longer time to grow [Sha12].

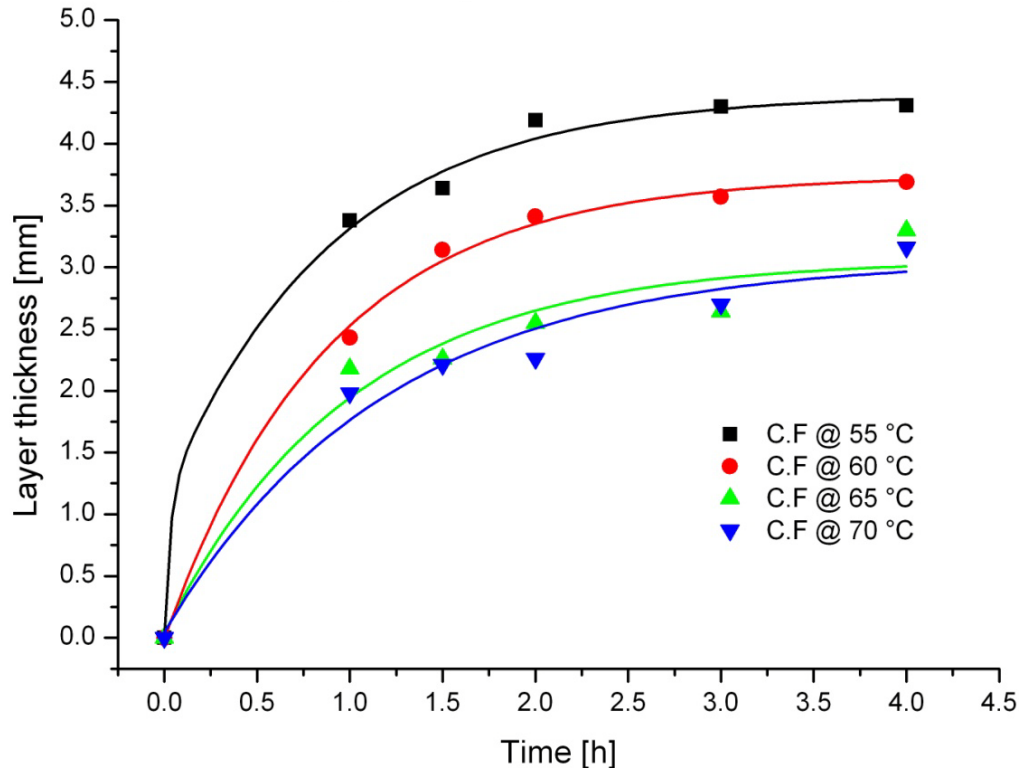


Fig. 5.3 Average layer thickness at different temperatures of the cold finger

5.1.3 Crystal growth rate at different temperatures as a function of layer thickness

The crystal growth of the layer was measured as a function of crystal layer thickness at different crystallization times. The average crystal growth rates are calculated by dividing a layer thickness with the crystallization time [Kim02]. As it is shown in Fig. 5.4 crystal growth rate is more at the beginning of each experiment, but it decreases gradually with the increase in crystallization time. The reason for this behavior is that at high cooling rates, the crystal growth rates are also high at the beginning. Due to fast crystal growth, the crystal layer thickness increases rapidly and as a result the heat flow resistances between the melt and cold surface also increases. This results in the decrease of crystal growth rate with increasing layer thickness and crystallization time [Bei12]. The low cooling rates lead to smaller growth rates and a moderate increase in heat flow resistances as shown in last two curves in Fig. 5.4 where the temperature of the cold finger were 65 °C and 70°C.

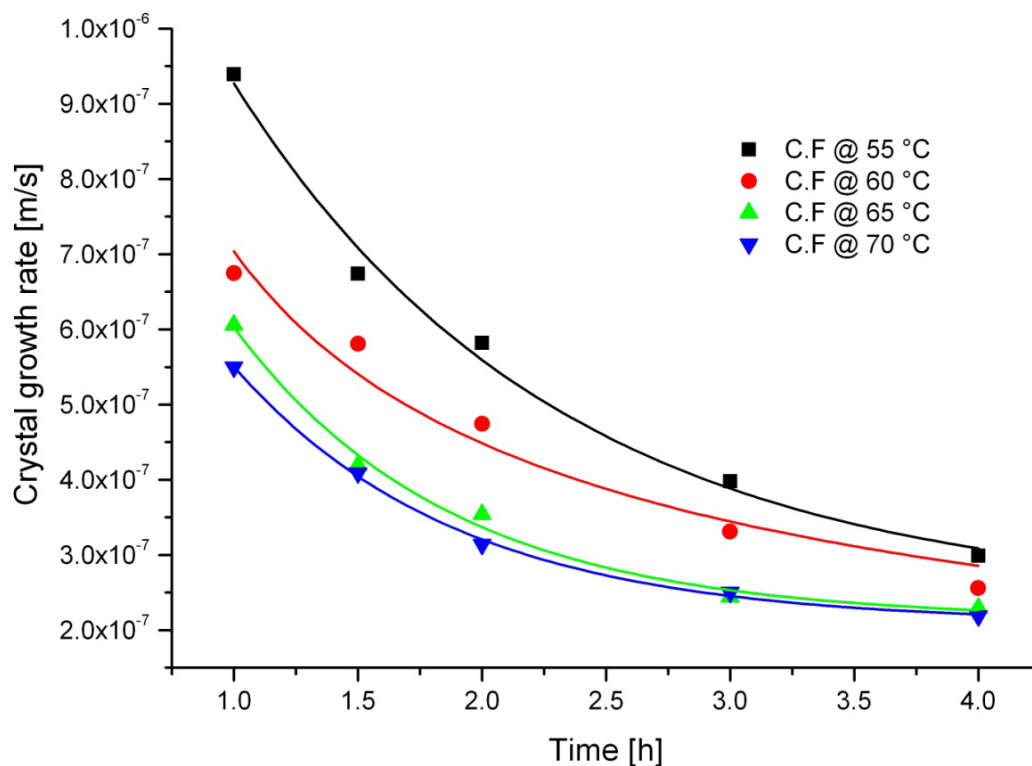


Fig. 5.4 Effect of crystallization time on average crystal growth rate

5.1.4 Effect of crystallization time on purity of the crystal layer

The initial concentration of the melt and crystal layer was measured by HPLC for different temperatures of the cold finger at the end of each experiment. These results show that the concentration of the layer increases with growing distance from the cold surface for a certain period of time as shown in Fig. 5.5. After 2 hours of the process, the purity of the crystal layer decreases due to adherence of impurities in the contaminated residual melt at the bottom of a crystallizer [Sch93].

The maximum value of the purity of the 5-isomer achieved is $96.6 \pm 0.3 \%$ at the temperature of $70 \text{ }^\circ\text{C}$, but at this temperature the crystal growth rate is also slow and it takes a longer time to grow as discussed before. At $60 \text{ }^\circ\text{C}$, the crystal growth rate is higher, but the layer with purity $95.8 \pm 0.3\%$ is formed which is low compared to the crystal layers at temperatures of 65°C and 70°C as shown in Fig. 5.5. At the high cooling rate, the growth rate of the crystal is also high and the amounts of impurities growing with crystal and melt inclusion adhering with crystal layer also become faster

[Sch93]. As a result purity of the layer decreases at high cooling rates with time, which is evident in Fig. 5.5.

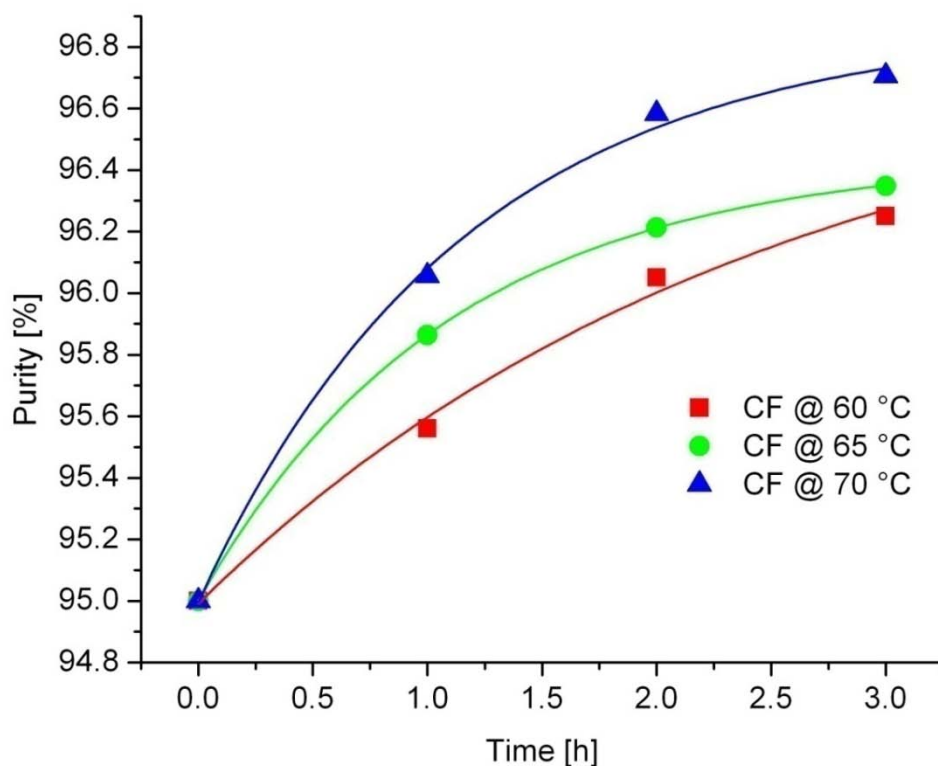


Fig. 5.5 Purity analysis at different temperatures of the cold finger

It is clear from these results that at higher cooling rates the purity of the layer is low while at the low cooling rate the purity is improved, but it takes long operation times which are not good for the economic reasons [Sha12]. Based on these result the cooling rate at the cold finger of 65 °C is selected for the further investigation in this work.

5.1.5 Purification by sweating

To check the effect of sweating on purification of the product, crystallization is done at a temperature of the cold finger at 65 °C for the different crystallization times as shown in crystallization curve in Fig. 5.6. Thereafter, the post-crystallization step “sweating” was performed for each experiment at different crystallization times, i.e., 1, 2 and 3 h one by one. The samples were taken at different time intervals during a sweating process and were analyzed by HPLC using method 1 for the purity. The upper three sweating curves

in Fig. 5.6 show the results from sweating analysis. Sweating needs a much shorter retention time of about one hour only in this case and is therefore faster as compared to the crystallization process of 3 hours. The samples were taken after 25 min for each individual crystallization time and were plotted in sweating curves. These results show that the purity of the layer increases with sweating because in sweating process material is heated gain near to its melting point for a short time, as a result the crystal layer re-melts again and the viscosity of these impurities adhering to the crystal layer decreases and are drained of under the influence of gravity as a sweating liquid [Ulr03b].

The maximum purity attained after the sweating process was about 98% of the 5-isomer and the percentage loss of the product during the whole process of crystallization and sweating was about 8%.

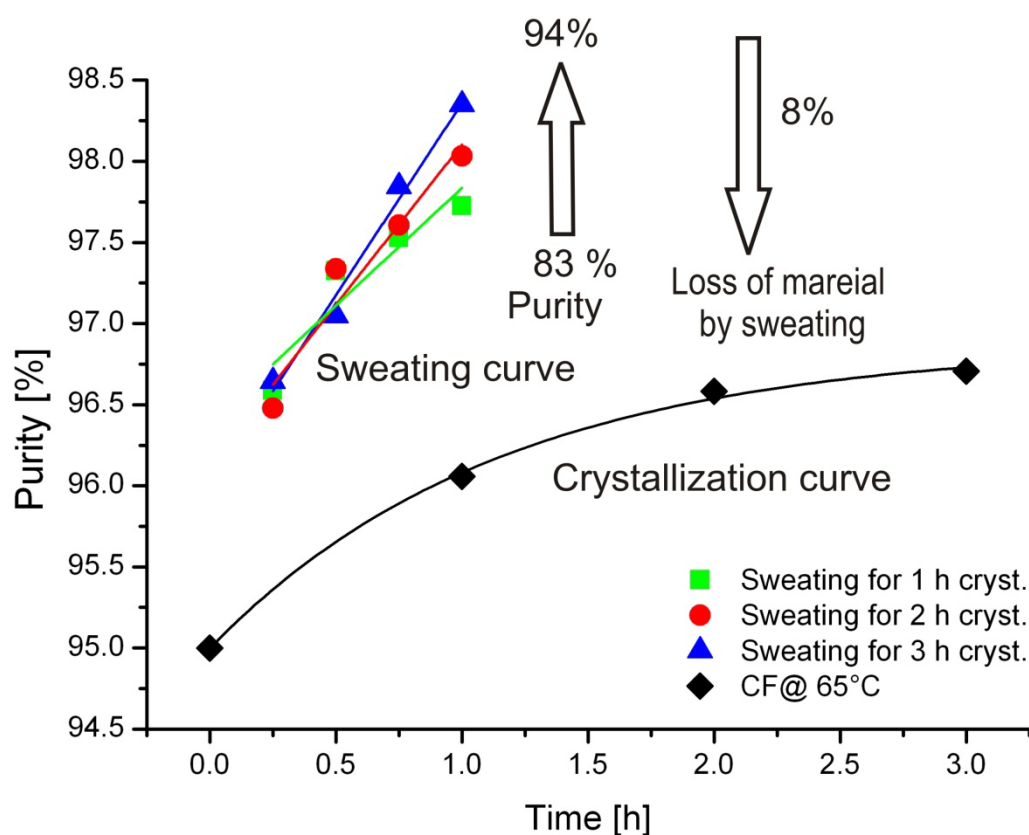


Fig. 5.6 Effect of sweating on crystallization purity and yield of the layer [Ahm15] [Ahm16]

5.1.6 Purification of residual melt

The product was purified successfully by a single step of layer melt crystallization up to 98% after sweating with the minimum loss of material. The problem with separating such a multi-component product is that the ratio of the different components can change during the process. In this case study, the ratio of the two isomers is reversed after crystallization at different temperatures of the cold finger as shown in Fig. 5.7. The 5-isomer begins to crystallize at a higher rate as compared to the 3-isomer what is opposite to the actual concentration of the product. The actual ratio of the 3-isomer is approximately 64 to 70% and the ratio of the 5-isomer is app. 34 to 30% in the product as given in the first bar of Fig. 5.7.

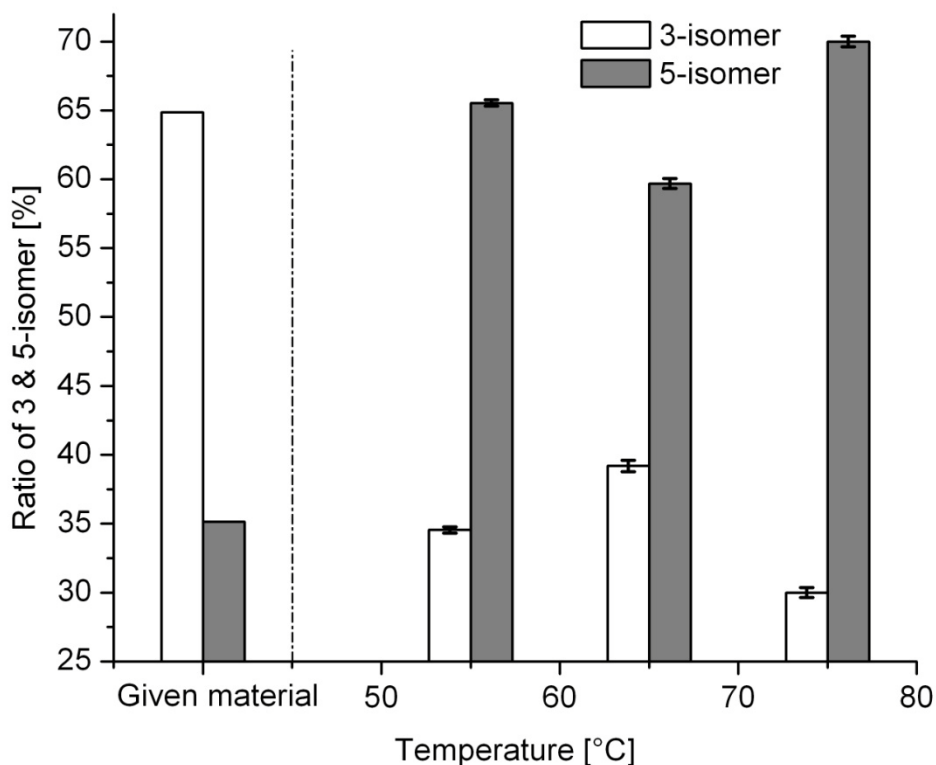


Fig. 5.7 Ratio of 3 and 5-isomers after separation [Ahm15] [Ahm16]

Therefore, to maintain the ratio of the 3 and 5 isomers constant with maximum possible purity in the final product (according to the product specification as it is to date after distillation) is the main task of this work. Hence, these two isomers are separated by recrystallizing the same residual melt in different crystallization stages.

The approach adopted to separate the two isomers is to recrystallize the residual melt into four different additional crystallization stages while the other conditions for experiments are kept constant for each stage of crystallization. The results with respect to the purity and the ratio of the isomers were measured for each step by using HPLC method 1 (for purity) and method 2 (for a ratio of isomers) respectively and were plotted in Fig. 5.8. In the end, all the fractions obtained from different stages were mixed together to check the overall effect of the purity and composition of the product whether it is according to the product specification or not.

Each time a crystal layer is grown on the cold surface for 3 h and then samples were taken for analysis. In the first batch, the maximum amount of approximately 65% of 5-isomer was crystallized from the mixture. After that, the remaining melt was further treated in different batches to crystallize the 3-isomer. The amount of the 3-isomer increases in each step as shown by the bars in Fig. 5.8 due to the increase in the concentration of the 3-isomer in the residual melt. The maximum concentration of the 3-isomer was achieved in the 4th step.

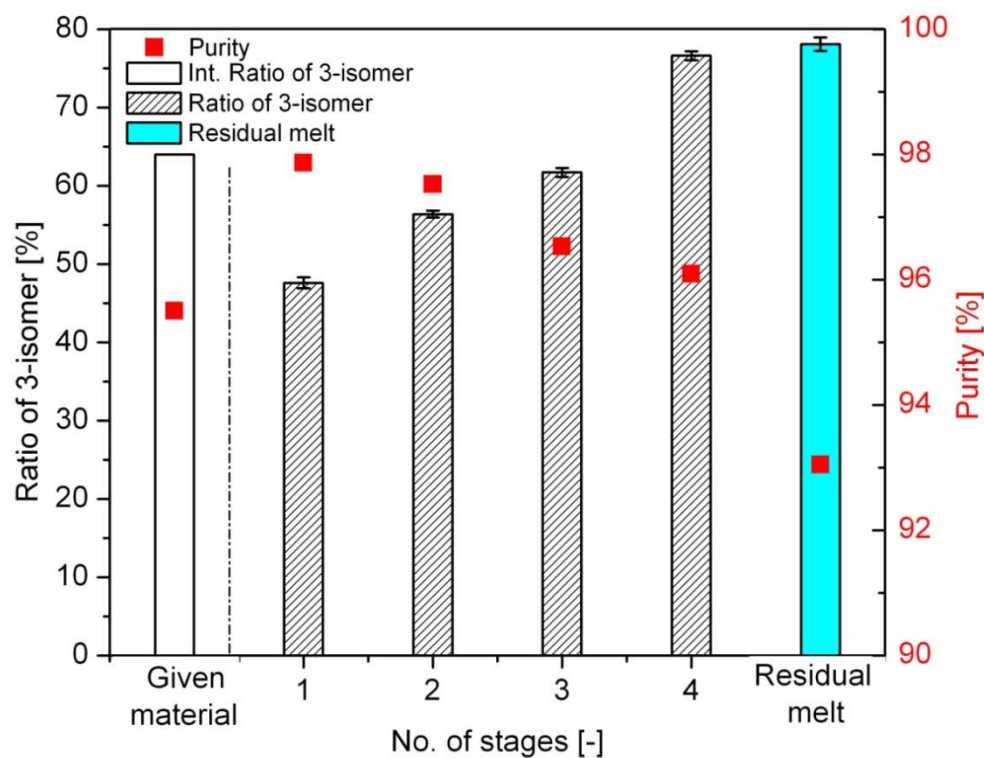


Fig. 5.8 Purification of residual melt into different crystallization stages with respect to the ratio of 3-isomer and purity of the product [Ahm15] [Ahm16]

In the mean time, the purity of the layer was also measured. The purity decreased slightly after each stage due to the increase in the amount of impurities in the residual melt as shown in the last bar in Fig. 5.8 The amount of the 3-isomer increases with increasing amount of the impurities in the residual melt. In the end, this residual melt can be recycled to the feed tank or wasted according to the demand.

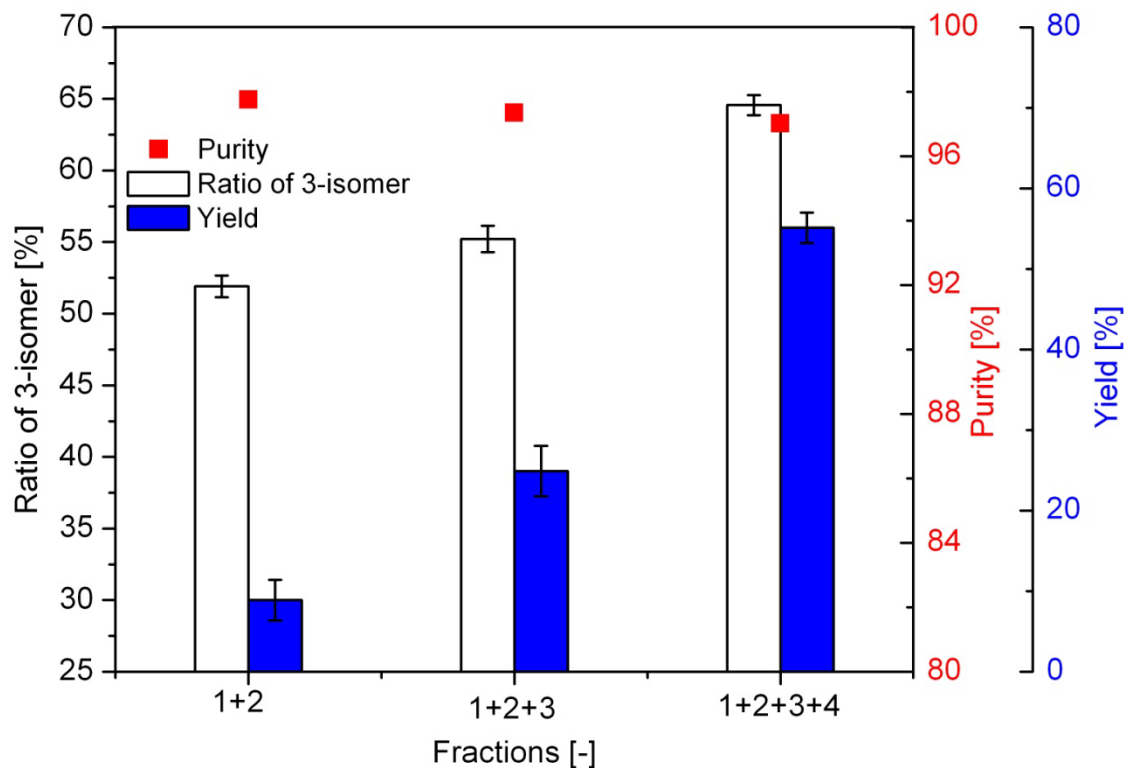


Fig. 5.9 Effect of mixing all different fractions on a ratio of 3-isomer, purity and yield of the product [Ahm15] [Ahm16]

After that, all fractions obtained from each batch with different ratios of isomers were mixed together. The effect of mixing all the fractions can be seen in Fig. 5.9. In each case, the purity remains almost the same, but there is an improvement in the concentration of the 3-isomer in the product and the yield of the process. By mixing all these fractions a product with the required specification can be produced with the maximum purity of about 97% (as compared to the purity obtained in a single step of crystallization which was 98%) and the right mixture of the isomers. This means to maintain the right mixture of the isomers, slightly compromise on the purity has to be made. The overall yield attained by this method is 60%, which can be increased further

if there is no restriction to maintain the ratio of these isomers. The effect of mixing the fraction on purity and yield can be seen in Fig. 5.9.

5.1.7 Crystal shape, habit and morphology

As crystallization is a very fast process and nucleation starts immediately after dipping a cold finger into the melt. It is difficult to study the crystal growth habit and morphology of these crystals during a crystallization process. The crystal morphology and habits of this product were therefore studied under a microscope (Keyence digital microscope (VHX500F)) to understand the growth mechanism of crystals of these materials.

A single stable nuclei (a very small crystal) is isolated during the crystal growth of the melt and studied under the microscope to check the crystal growth habit for 6 min. Tetrahedral shaped crystal forms in a supersaturated system and its size increases with a time to grow into the crystals of significant size as shown in Fig. 5.10. In melt crystallization mass transfer plays a very important role in crystal growth. During the mass is transferred from the bulk of the melt to the crystallizing component's surface of a crystal and latent heat transfer from the surface of the crystal to the bulk of the melt in heat transfer [Chi03].

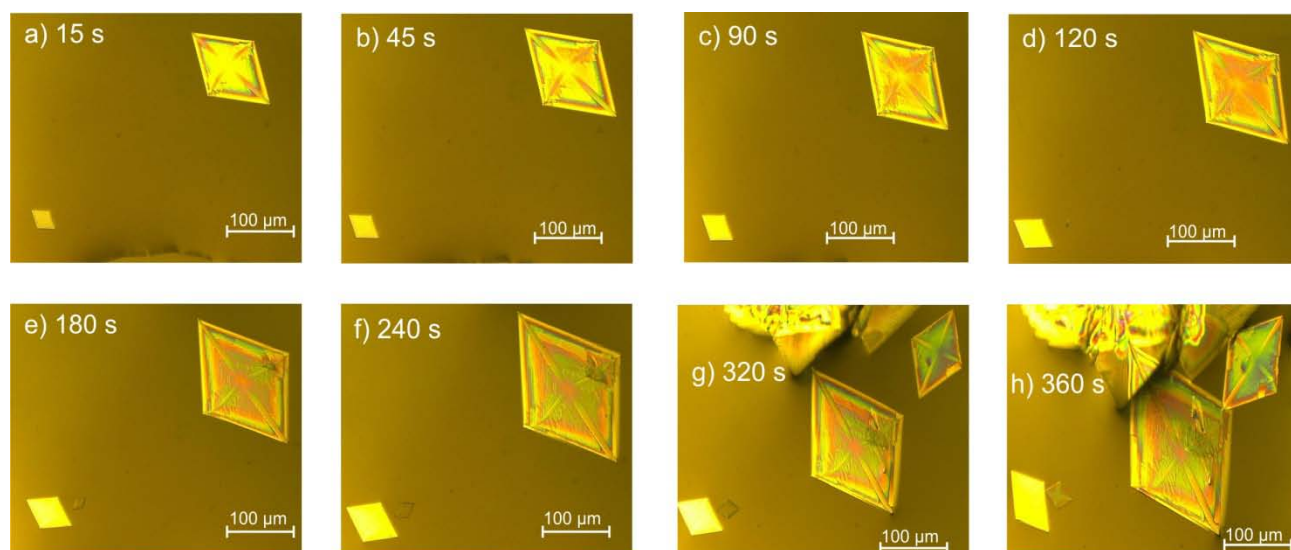


Fig. 5.10 Crystal growth at different times: a) 15 s; b) 45 s; c) 90 s; d) 120 s; e) 180 s; f) 240 s; g) 320 s; h) 360 s

5.2 Case study II '3-isomer'

5.2.1 Solid-liquid equilibrium

To check the feasibility of separation of 3-isomer by layer melt crystallization, the solid-liquid equilibrium between 3-isomer and 5-isomer was measured again by taking the different ratio of these isomers by using DSC. The onset temperature was used to calculate the solidus and liquidus curves.

All these values were plotted together to get the binary eutectic phase diagram of the system between the 3-isomer and the 5-isomer. The liquidus lines of the system intersect at the value of 0.1 wt.% of the 5-isomer and give the eutectic point. These results clearly show that this system is a simple binary eutectic system with a eutectic point at a composition of 0.1 ± 0.03 wt.%. with the eutectic temperature at approximately 88 °C. In Fig. 5.11 the red line represents the melting curve of the 5-isomer measured experimentally by DSC while the black lines represent a melting curve of the 3-isomer. All these values were measured three times with a standard deviation of about 5%. The yield of the process calculated theoretically by the phase diagram and is found to be about 90%.

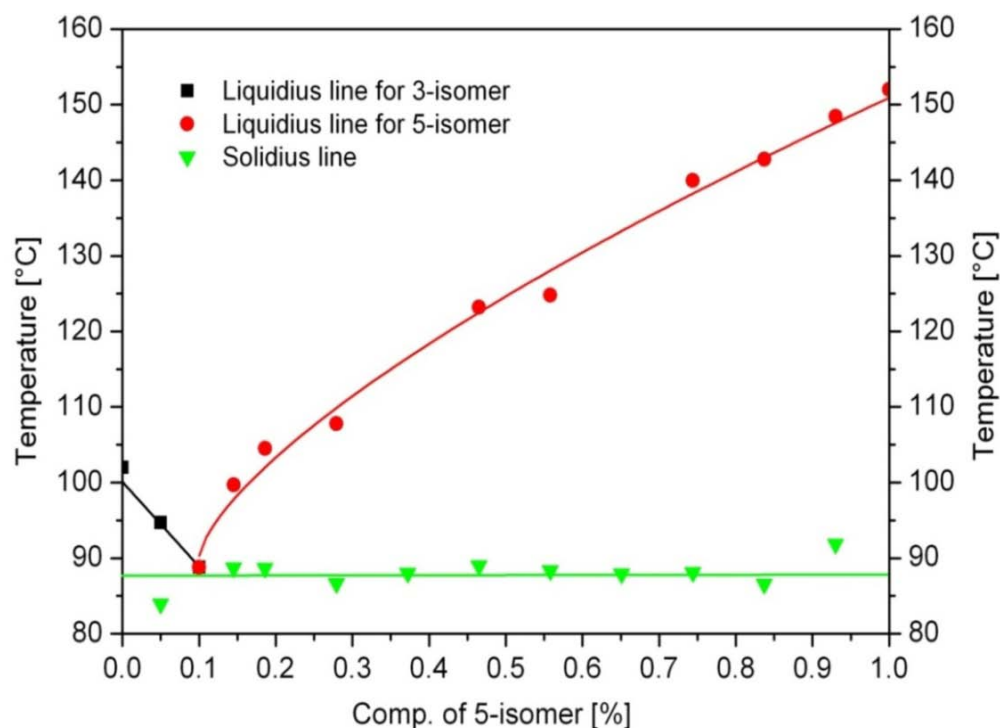


Fig. 5.11 Binary eutectic phase diagram between 3-isomer and 5-isomer

5.2.2 Purity of the layer

After that, to check the effect of purity of the 3-isomer the crystallization was carried out again in a lab scale solid layer melt crystallizer by taking a 25 g of the 3-isomer. This system is measured as a pure binary system in which the 3-isomer is considered as pure components while all other components were considered as impurities. It has a purity of 83% and contains 14% of 5-isomer and 3% of impurities. The purity of the melt and crystal layer was measured by HPLC using method 1 for different crystallization times at the cold finger temperature of 60 °C at the end of each experiment.

It can be observed from the crystallization curve in Fig. 5.12 that there is an increase in the purity of the layer after each experiment for different crystallization times. The purity of the layer increases with time and then becomes almost constant after 3 h which is evident from the first crystallization curve. The maximum purity achieved after crystallization for 3 h was $87 \pm 0.3\%$.

Thereafter, the post-crystallization step “sweating” was performed again for each experiment at different crystallization times one by one as shown in the sweating curves in Fig. 5.12. The maximum purity attained after the sweating process is about 94% and the percentage loss of the product during the whole process of crystallization and sweating is about 7%.

Consequently, the final purity of the layer is increased from 83% to 94% in a single step of purification and the percentage loss of the final product was about 7% after sweating which is in an acceptable range.

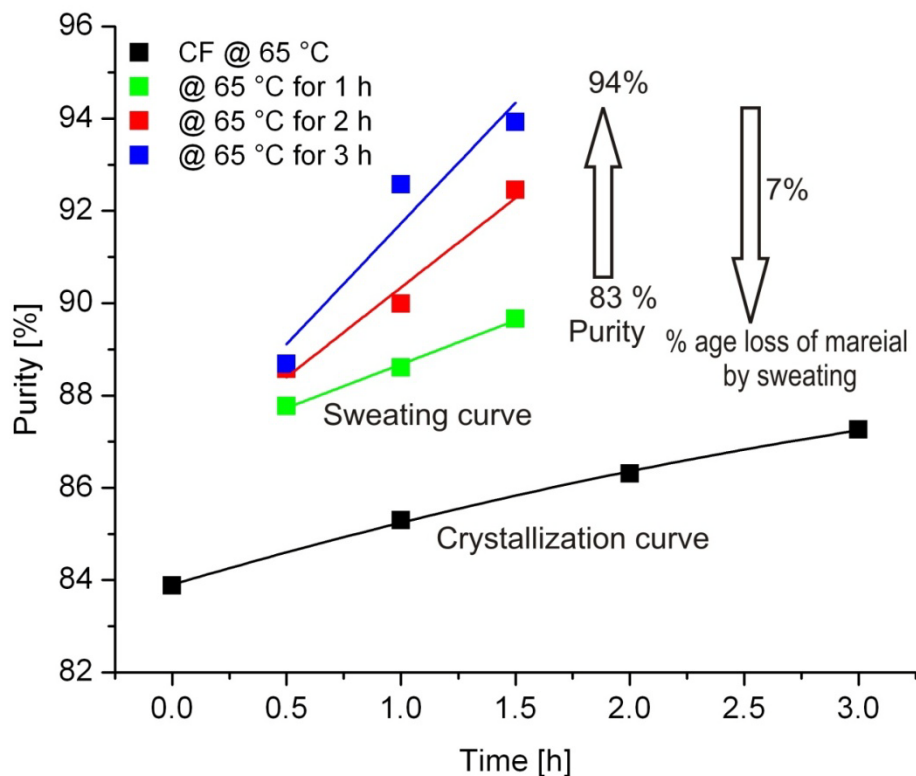


Fig. 5.12 Effect of crystallization time on purity of 3-isomer crystal layer

5.2.3 Residual melt treatment

In the end, to verify the ratio of the 3 and 5 isomers in the final product, the residual melt is treated in three different batches. The actual ratio of the 3-isomer is approximately 83% as shown in the first bar in Fig. 5.13 and the ratio of the 5-isomer is app. 14% in the product. The purity and ratio of the isomers were measured together and were plotted in Fig. 5.13. There is no problem of a change in the ratio of 3 and 5-isomers is observed. Actually, the final ratio of the 3-isomer is increased in the final product from 87% to 91%. This result in an increase of the overall purity of the product because in this case the 5-isomer was also considered as an impurity and the overall purity of the product remained almost constant in each batch.

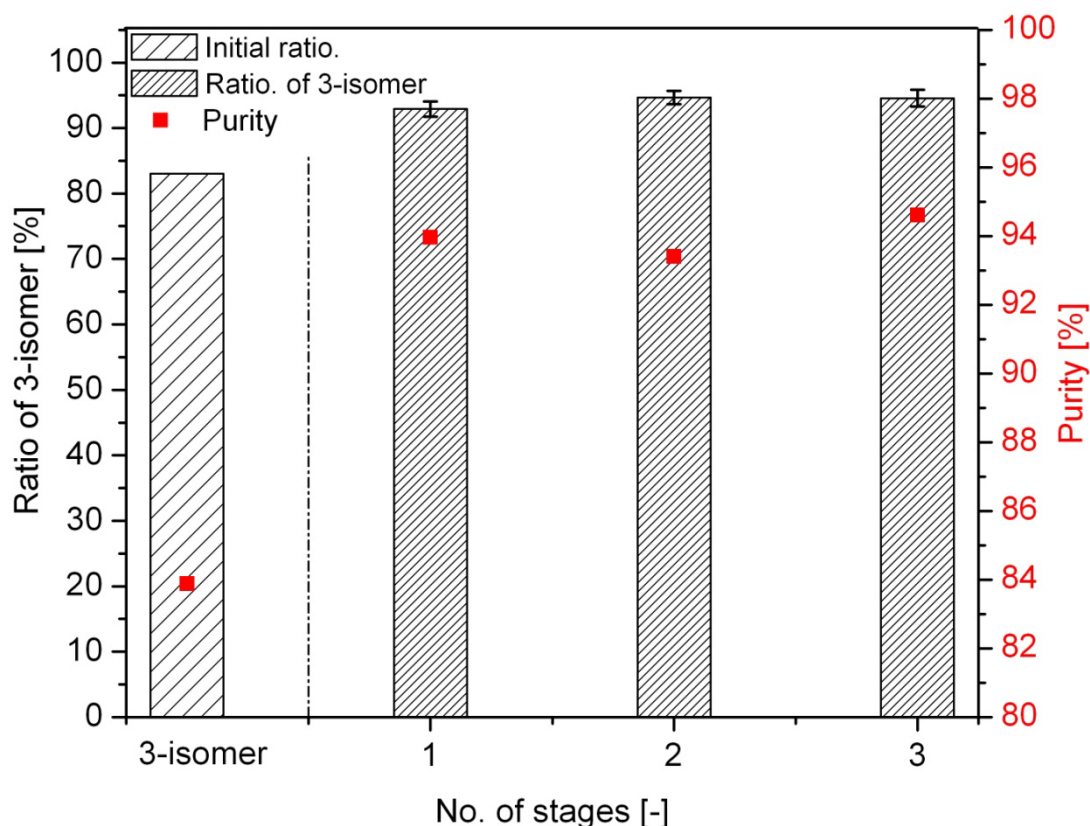


Fig. 5.13 Purification of residual melt into different batches with respect to the ratio of 3-isomer and purity of the product

5.3 Calculation of phase change energies

5.3.1 Enthalpy of vaporization

To find the phase change energies a TGA-DSC is used simultaneously. This combined technique helps us to measure the heat of fusion and vaporization directly. The heat flow 'Q (J)' is measured by the DSC isotherm while the total mass loss 'm (g)' during the process is measured from the TGA. As shown in Fig.5.14. The values of Q_{fus} (J) and Q_{sub} (J) are measured by taking the areas the respective peaks starting from their onset temperature from DSC curves as described in Fig. 5.14 and the amount of mass loss 'm (g)' is obtained from the TGA curve. These values are substituted in Eqs. 5.2 and 5.3 to calculate the values of enthalpy of fusion and vaporization in this work.

$$\Delta H_{\text{vap}} = Q/m = J/g \quad \text{Eq. 5.2}$$

$$\Delta H_{\text{fus}} = Q/m = J/g \quad \text{Eq. 5.3}$$

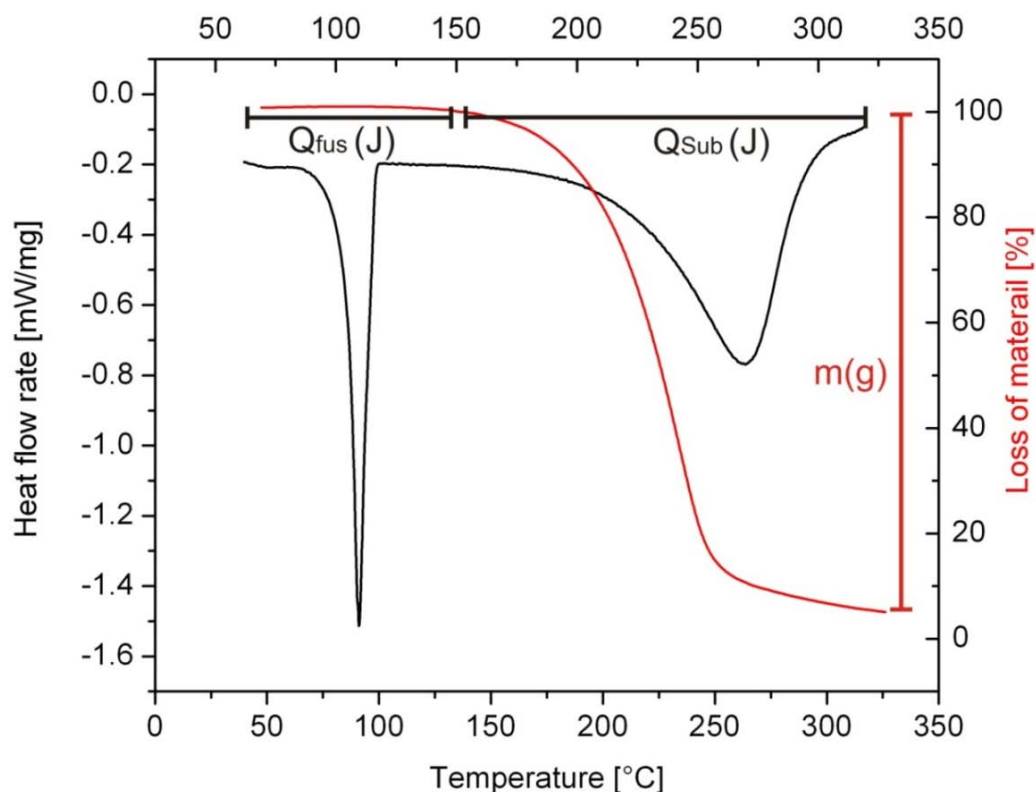


Fig. 5.14 TGA-DSC curves for measuring heat of fusion and vaporization

The enthalpy of vaporization is measured if the substance is in the liquid phase and for the solid substances the heat of sublimation is used in these calculations. The enthalpy of sublimation can be divided into two steps. First, melting of the solid into the liquid and then the liquid into the vapor phase and the combinations of these two values gave the value of heat sublimation [Tau09] [Pet07].

$$\Delta H_{\text{fus}} + \Delta H_{\text{vap}} = \Delta H_{\text{Sub}} \quad \text{Eq. 5.4}$$

The other important advantage of TGA-DSC method is that it also gives the direct information about the stability of the product (whether it is decomposing or not) during a TGA analysis over a high range of temperature. In this work all the products used are

stable up to their boiling point and heat of vaporization is calculated at the boiling temperature.

5.3.1.1 Benzoic acid

The benzoic acid is taken as a standard material for the calibration of TGA-DSC because it is a solid material and its thermal data necessary for the calculation of phase transformation energy is also available in the literature. This literature data can be compared with the calculated values to check the validity of this method. The benzoic acid is a special material it sublimates below the melting point and it evaporates above the melting point. The heat of sublimation and vaporization for the benzoic acid are calculated from the TGA-DSC isotherms. The results for the analysis of benzoic acid are plotted in Fig. 5.15.

The heat of sublimation calculated from TGA-DSC curves is -751.25 J/g and the literature value extrapolated from the work of Robert de Silva [Sil04] is -742 J/g. After that, the value of the heat of vaporization -596.033 J/g is calculated by using the Eq. 5.3 and is compared with value -630 J/g in the work of Sauerbrunn [Sau09] where he has calculated the heat of vaporization by using TGA-DSC simultaneously.

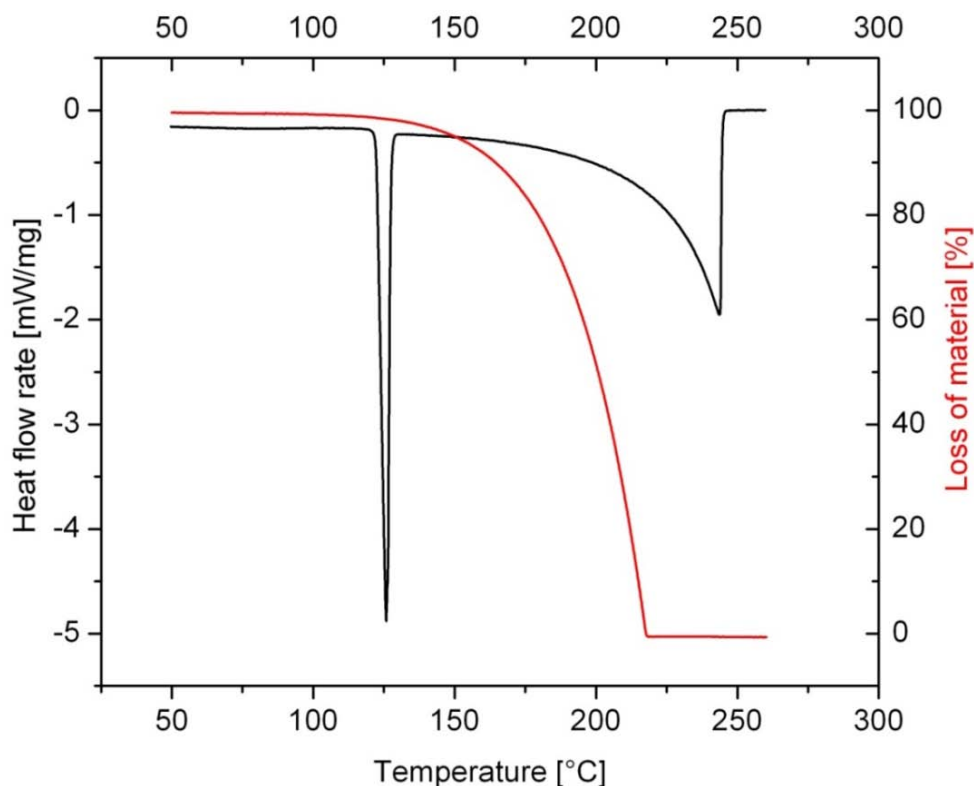


Fig. 5.15 TGA-DSC curve for benzoic acid

The above results show that all the values obtained from experiments are comparable with literature as given in Tab. 5.1 and this method can be used for the further analyses of the product 'A' and 3-isomers.

Tab. 5.1 Values for heat of sublimation and vaporization for benzoic acid

Enthalpy of	Measured value [J/g]	Literature value [J/g]	Difference [%]
Sublimation	- 751	- 742 [Sil04]	2
Vaporization	- 596	- 630 [Sau09]	6

5.3.1.2 Raw Product 'A'

Clausius-Clapeyron equation is a very important equation to measure the enthalpy of vaporization of the components. This equation is used mostly by the scientist to measure the vapor pressure or heat of vaporization of pure liquids and solids substances. The enthalpy of vaporization for the product 'A' is calculated first by

Eq. 5.5. It will give the first estimation about the magnitude of the enthalpy of vaporization value of the product which will be used later to calculate the phase change energy.

$$\ln \left[\frac{P}{P_0} \right] = - \frac{\Delta H_{\text{vap}}}{R} \left[\frac{1}{T_2} - \frac{1}{T_1} \right] \quad \text{Eq. 5.5}$$

P is the vapor pressure and P_0 is the vapor pressure at standard temperature and ΔH_{vap} is the enthalpy of vaporization in the case of liquid substances or enthalpy of sublimation for solid substance. The value of P (20 °C) = 0.0356 Pa and P_0 (25 °C) = 0.0624 Pa is provided in the product data sheet at their specific temperatures.

The isotherms for the TGA-DSC analysis of the Product 'A' are shown in Fig. 5.16. The heat of the fusion is calculated from the first melting peak and heat of sublimation is calculated from the second peak. There is also no decomposition observed during the heating of the material, the loss of the mass is due to the sublimation of the product when the temperature is approaching the boiling point.

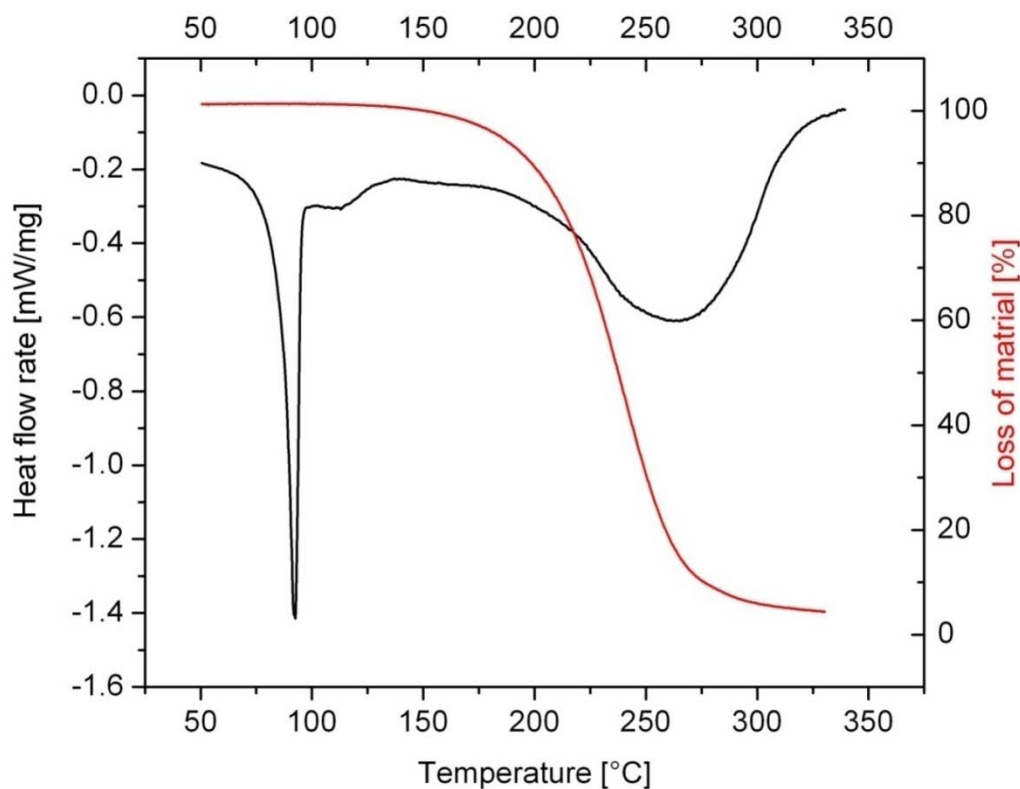


Fig. 5.16 TGA-DSC curve for product 'A'

The value of the heat of sublimation, calculated by the Clausius-Clapeyron equation, is - 600 J/g and it is compared with the value measured from TGA-DSC method which is - 610 J/g. The comparison between the calculated and measured values seems to be in good agreement and is given in Tab. 5.2.

Tab. 5.2 Values for enthalpy of vaporization for product ‘A’

Enthalpy of vaporization	Measured value [J/g]	Calculated value [J/g]	Difference [%]
		610	600

The values of the heat of fusion and sublimation of all the products measured by TGA-DSC method is summarized in Tab.5.3.

Tab. 5.3 Enthalpy of fusion and vaporization for all material measured by TGA-DSC

Material	Melting point [°C]	Heat of fusion [J/g]	Boiling point [°C]	Heat of vap. [J/g]
Benzoic acid	122.41	- 164.93	250	- 596.03
Product ‘A’	94 -122	- 138.2	270.7	- 610.3
3-isomer	102 - 104	- 139.35	215	- 453.6

5.3.2 Phase change energies

After that, the amount of energy needed to transform the liquid phase to solid in crystallization and liquid phase to the gas phase in distillation is calculated from the enthalpy of fusion and vaporization (measured by the above mentioned method) by using Eq. 5.6 and Eq. 5.7. These values are compared together by taking the same amount of the material crystallized during the layer melt crystallization to check the feasibility of this method.

$$Q = m\Delta H_{fus} \tag{Eq. 5.6}$$

$$Q = m\Delta H_{vap} \tag{Eq. 5.7}$$

The calculated values for the heat of crystallization and distillation are given in Tab.5.4. This table shows that heat of transition for crystallization is 2 to 5 times smaller than in distillation for both products [Bra86] and 70 to 75 % of the energy can be saved by melt crystallization compared to distillation [Win94].

Tab. 5.4 Amount of energy required during crystallization and distillation

Material	Q for Cryst. [KJ]	Q for Dist. [KJ]	Energy saving [%]
Product 'A'	- 2.683	- 12.418	78
3-isomer	- 2.475	- 8.125	69

6. Discussion

In this Chapter, all the results demonstrated in Chapter 5 are discussed in detail and the comparisons with existing data are also made. The available literature with reference to the results will be discussed for the observed facts. The reasons behind the effects of the temperature, crystallization time and supersaturation will be given and the use of the technique on broader canvas will be shown.

6.1 Case study I 'Raw Product 'A''

6.1.1 Solid-liquid equilibrium

The solid-liquid phase diagram provides fundamental thermodynamic data necessary for the purification of materials by melt crystallization. Therefore, to construct the solid-liquid equilibrium phase diagram, DSC was used by measuring the melting points of several samples at different composition. The results obtained from DSC for all samples at different composition are shown in Fig. 5.1.

The results of the DSC experiments give an isotherm of heat flux and temperature. The enthalpy of fusion (ΔH_f) and melting point (MP) is measured simultaneously from these curves. An endothermic phase change gives a negative peak while exothermic peak results in a positive peak. The area of the peak gives the value of the heat of fusion and melting point is measured from the onset temperature of the peak. The pure samples give sharp peaks while samples with the mixture of components show a broader peak as it is evident in the isotherm of product 'A' in Fig. 5.1. This product is a mixture of 3 and 5 isomers with some impurities. Two different exothermal peaks are observed in all the cases of a binary mixture of different composition. The first peak at the lower temperature is caused by a phase change from the solid state to a two-phase system with the solid and liquid at eutectic composition. The second peak at higher temperature shows the transition from solid-liquid to complete melt for the major component [Hen10].

The liquidus curve for the binary system of the product 'A' and 5-isomer represented by the black line in Fig. 5.2 is interpolated by using the Schröder-van-Laar equation. The first peak with lower temperature in DSC curves corresponds to the melting of the

eutectic mixture and is used to construct the solidus line. While the second peak with the higher temperature is a characteristic of the liquidus equilibrium curve or melting point of the major component. These calculated values of the solubilities for the product 'A' and 5-isomer are calculated with Eq. 5.1. The calculated values are compared with the values obtained experimentally by DSC. These calculated and experimental values are found to be in good agreement with each other with a standard deviation of approximately 5%.

The liquidus line marked the solubility of one component into the other at equilibrium. The liquidus line in the phase diagram describes the equilibrium state between the liquid and solid phase. A phase change (from liquid to solid) can be achieved if the system is brought into a non-equilibrium state due to the driving force. In the case of melt crystallization, the under-cooling of the melt is the driving force for nucleation process. This under-cooling can be achieved up to a certain temperature by inserting the cold finger into the melt. In this way, the temperature of the melt is decreased below the liquidus line. Therefore, the nucleation starts at a temperature lower than the liquidus temperature theoretically. The temperature ranges between the liquidus line and temperature at which nucleation start is known as a metastable zone width as shown in Fig. 6.1. It is a maximum supersaturation (under-cooling) achievable before crystallization (nucleation) starts. The metastable zone width depends on melt concentration, fluid dynamics in the melt vessel and cooling rate [Chi03].

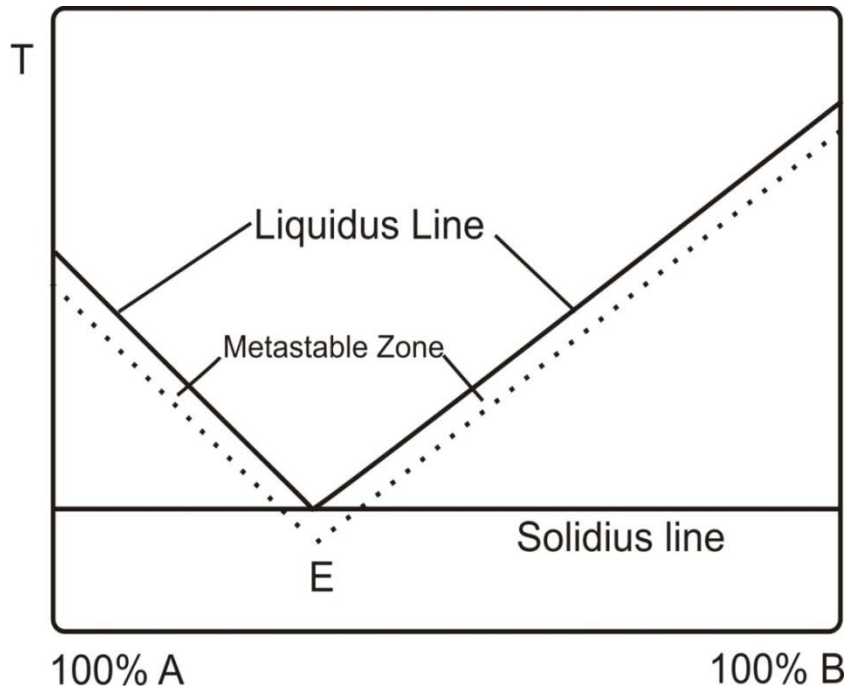


Fig. 6.1 Simplified phase diagram of eutectic system

6.1.2 Effect of crystallization time on crystal growth rate at different temperatures

In this section, the effect of crystallization time on crystal growth is studied at different temperatures of the cold finger (cooling rates) as a function of crystal layer thickness. The crystal growth rates are measured at different cooling rates by changing the temperature of cold finger. The layer grows quite fast at the beginning and then its growth rate decreases continuously until a certain layer thickness is attained as shown in Fig. 5.4. The average crystal growth rates are calculated by dividing the layer thickness by the crystallization time [Kim02]. The thickness of the crystal layer formed on the surface of the cold finger mainly depends on the growth rate and is expressed as a function of time in growing the layer. The crystal growth is defined as a change in the thickness of the layer ' ΔL ' during the time interval ' Δt ' [Kim03]. In layer melt crystallization, a driving force for crystal growth is the degree of sub-cooling. It is the mean temperature difference between the melt and the equilibrium temperature in front of the crystal layer (in this case temperature of the cold finger) [Kim03][Bei12].

The growth rate increases with increasing in the cooling rate because the driving force for crystal growth, the temperature difference between the melt and cold finger is high. This effect can be seen in first two curves of Fig. 5.4 where the temperature of the cold finger is 55 and 60 °C and layer growth is fast due to the high degree of supersaturation (ΔT).

At a moderate cooling rate, the growth rate shows a linear dependency on the layer thickness. This can be explained by the heat flow resistances of a crystal layer. At high cooling rates, the growth rates are also high at the beginning and a rapid increase in heat flow resistances. This would result in a fast increase in crystalline layer thickness followed by a decrease in crystal growth rate. It would also result in an increase in thermal conductive resistance of the crystalline layer due to an increase in thermal resistance of the layer [Bei12]. Whereas, a low cooling rate results in a slower growth rate and the layer needs a longer time to grow with a moderate increase in thermal resistances. The description can be seen in last two curves in Fig. 5.4.

6.1.3 Effect of crystallization time on purity of the crystal layer

The initial concentration of the melt and crystal layer is measured by HPLC for different temperatures of the cold finger at the end of each experiment. These results show that the concentration of the layer increases with growing distance from the cold surface for a certain period of time as shown in Fig. 5.5. It also suggests that most of the impurity inclusions are entrapped at the beginning of the crystallization process due to the high degree of supersaturation [Kim03]. After 2 h of the process, the purity of the layer decreases due to adherence of impurities in the contaminated residual melt at the bottom of a crystallizer.

As discussed in Chapter 6.1.2, the cooling rates affect the crystal growth rate and the crystalline layer formed at different cooling rates leads to different amounts of liquid inclusion and in cooperated impurities. It is clear from the results shown in Fig. 5.5, at fast cooling rates the temperature between the melt and cold surface increases as a result of which the degree of supersaturation increases and of a porous layer with high growth rate and concentration of impurity is produced. Whereas, at low cooling rates a

compact structured layer is produced with the improved purity when the temperature of the cold finger is at 65 and 75 °C, but it takes longer operation times which are not favored due to the concerning economic reasons [Well94] [Kim01] [Sha12].

For high purification of the crystalline layer, a combination of both methods i.e., crystallization and sweating for an improvement of the purity of the crystalline layer even at higher growth rates, however, with some product loss.

6.1.4 Purification by sweating

To further increase the purity of the crystal layer, the post-crystallization step sweating is carried out at a temperature of 65 °C for different crystallization time instead of second crystallization step. The sweating process has some advantages over the second crystallization step [Ulr03b].

- The retention time of the process is usually shorter. It is about one-third (1/3rd) of the time of a crystallization step which means less energy consumption.
- No additional heat is needed for phase transition and hence the subsequent amount of the energy is saved as the product is partially melted.
- A product loss is also less during the sweating, which results in a better yield of the overall process.

It is a temperature induced purification step and the temperature of the cold finger is hereby raised near to the melting point of the pure product. In this case, the sweating is conducted at 10 degrees below the melting point of the pure compound. As mentioned above, the retention time is short for sweating, therefore, sweating process is carried out for 1 h and samples are taken for every 15 mins for the purity analysis. These results for sweating are shown in the upper three sweating curves in Fig. 5.6. The sweating curves in Fig. 5.6 show that the purity of the crystal layer increases in the first 40 min of the sweating operation. The impurity formed in the growing crystal is mostly located on the surface of the crystal layer. The impure inclusions entrapped on the outside layer are easy to be drained away at the beginning of the sweating. After 1 h,

the crystal layer purity has almost become constant, although sweating operation is still at work [Kim02].

The mechanism of purification by sweating can be explained by the fact that in the crystalline layer inclusions moved towards the surface of the layer. A higher temperature induced by sweating leads to a lower viscosity of the inclusions and a high porosity of the crystal layer, which promotes the impurities and inclusions to drain out under the influence of gravity as a sweating liquid [Bei13] [Kim02].

At the end of the process, the pure crystal layer is melted after the sweating to remove it from the surface of the cold finger. There is no extra energy needed for the phase transformation to remove the layer from the cooling surface, as the crystal layer is already partially melted due to the sweating. Hence, a certain amount of the energy can be saved.

To find the optimum sweating process conditions, it is not only sufficient to know the degree of purification by the sweating process, but also the amount of product loss which is characterized by the loss in yield 'Y'. The percentage loss of the material during the sweating is about 8 % in this work as shown in Fig. 5.6, which is comparable with data reported by Jancic in 10th Symposium on Industrial Crystallization according to which product loss is about 10% during the sweating process [Jan87] [Ulr03b]. The decrease of the yield is more at the beginning of the process and it's getting less with the increase in sweating time because first adherent melt drains out of the surface layer and then draining of the trapped inclusion starts later.

The overall purity of the product is increased from 95% to approximately 98% in a single step of crystallization and sweating. This increase of 3% in the overall purity of 'product 'A' after layer melt crystallization is not possible to achieve by a distillation process. It means the combination of crystallization and sweating has higher purification efficiency and less energy consumption as compared to the distillation.

6.1.5 Purification of residual melt

The product was purified successfully by a single step of layer melt crystallization up to 98% as discussed above after sweating with the minimum loss of material, but with some problems. The first is the yield of the crystallization step and the second is the ratio of the two isomers in the final product. The ratio of the two isomers is reversed after crystallization at different temperatures of the cold finger as shown in Fig. 5.7. The 5-isomer crystallizes more compared to the 3-isomer which is opposite to the actual concentration of the product due to the eutectic nature of these two isomers as shown in the phase diagram between 3 and 5-isomer in Fig. 5.11. The reason is that the initial concentration of the product is 64% of the 3-isomer and 36% of the 5-isomer. This concentration lies on the right side of the phase diagram where the liquidus line of 5-isomer is present as shown in Fig. 5.2. Therefore, 5-isomer began to crystallize more along the liquidus curve of 5-isomer compared to the 3-isomer till the eutectic point is reached.

Thus, to maintain the ratio of the 3 and 5 isomers constant with maximum possible purity in the final product according to the product specification, the residual melt is recrystallized in four different batches to separate the two isomers (not to purify them). In this method, one isomer is taken as a pure component and separated in first crystallization step while others are considered as an impurity and treated later in a further crystallization stage just like a binary mixture system as shown in Fig. 5.8. In the first batch, the maximum amount of 5-isomer is crystallized from the mixture with the purity of about 97%. After that, the remaining melt is further treated in different batches to crystallize the 3-isomer. The amount of the 3-isomer increases in each batch as shown by the bars in Fig. 5.8 due to the increase in the concentration of the 3-isomer in the residual melt. With the increase in the concentration of 3-isomer with each batch, the slight decrease in the purity of the layer is observed because of the increase in the amount of impurities in the residual melt and these impurities stick on the surface of the layer.

Finally, these separated streams with a high purity and different ratio of 3 and 5-isomer are mixed together to get the right mixture of the isomers and high purity of the overall

product according to the demand. By mixing all these fractions a product with the required specification can be produced with the maximum purity of about 97% (as compared to the purity obtained in a single step of crystallization which was 98%) and the right mixture of the isomers. This means to maintain the right mixture of the isomers, we have to compromise slightly on the purity. Hence, this method has following benefits as compare to other unit operations. (1) It gives an alternative route for the separation of the complex mixture of the different material by separating them in different stages. (2) There is the degree of freedom to mix 3 and 5-isomer together in different ratios which are more economically suited according to the demand.

6.1.6 Yield of the process

The overall yield of the process attained by this method is 60% and is plotted in Fig 5.9 which is relatively low as compared to the original process due to some limitations. The first problem is that there is a restriction of maintaining the ratio of 3 and 5-isomers in the product and the second is the interfacial area available for the crystallization which is also limited in this lab scale crystallizer.

It can be improved further if there is no restriction for maintaining the ratio of these isomers or by increasing the melt crystallization active area. Since the upper limit for melt-crystal for crystallization is in order of $10^2 \text{ m}^2/\text{m}^2$. This can be done by changing the design of the cold finger for crystallization. For example, by increasing the diameter of the cold finger or by increasing the rough surface on the cold finger in a well-defined manner. In this way, the overall surface area available for crystallization can be increased without changing the setup of the experiment.

These experiments are conducted in a lab scale crystallizer where the cold finger is used as a cooling surface for crystallization. It gives an idea about the feasibility of the purification process by static layer melt crystallization and predetermines the optimum operating parameter necessary for the industrial design and sizing phases. But in commercially available crystallizer by Sulzer and Proabd, a large number of parallel plates are used as the cooling surface for the crystallization. The active surface area available for crysallization can be adjusted according to the process. This means high yield can be obtained in these industrial scale crystallizers.

On the basis of the above discussion, the process flow scheme (state of the art) of the complete process for separating the 3 and 5-isomer into different stages and then mixing them together to fix the ratio of these isomers in the final product is shown in Fig. 6.2. This process flow diagram also gives the complete overview on the separation of the isomers after each stage, the purity of the final product and yield of the process. The yield of the 3-isomer is approximately 60% during the whole process which can be further increased if there is no restriction of maintaining the ratio of isomers.

**Feed (3-iso. + 5-iso.) = 95%,
(3-iso. = 64%, 5-iso. = 34%)
Imp = 5%**

3-iso. = 3-isomer
5-iso. = 5-isomer
Imp = Impurities

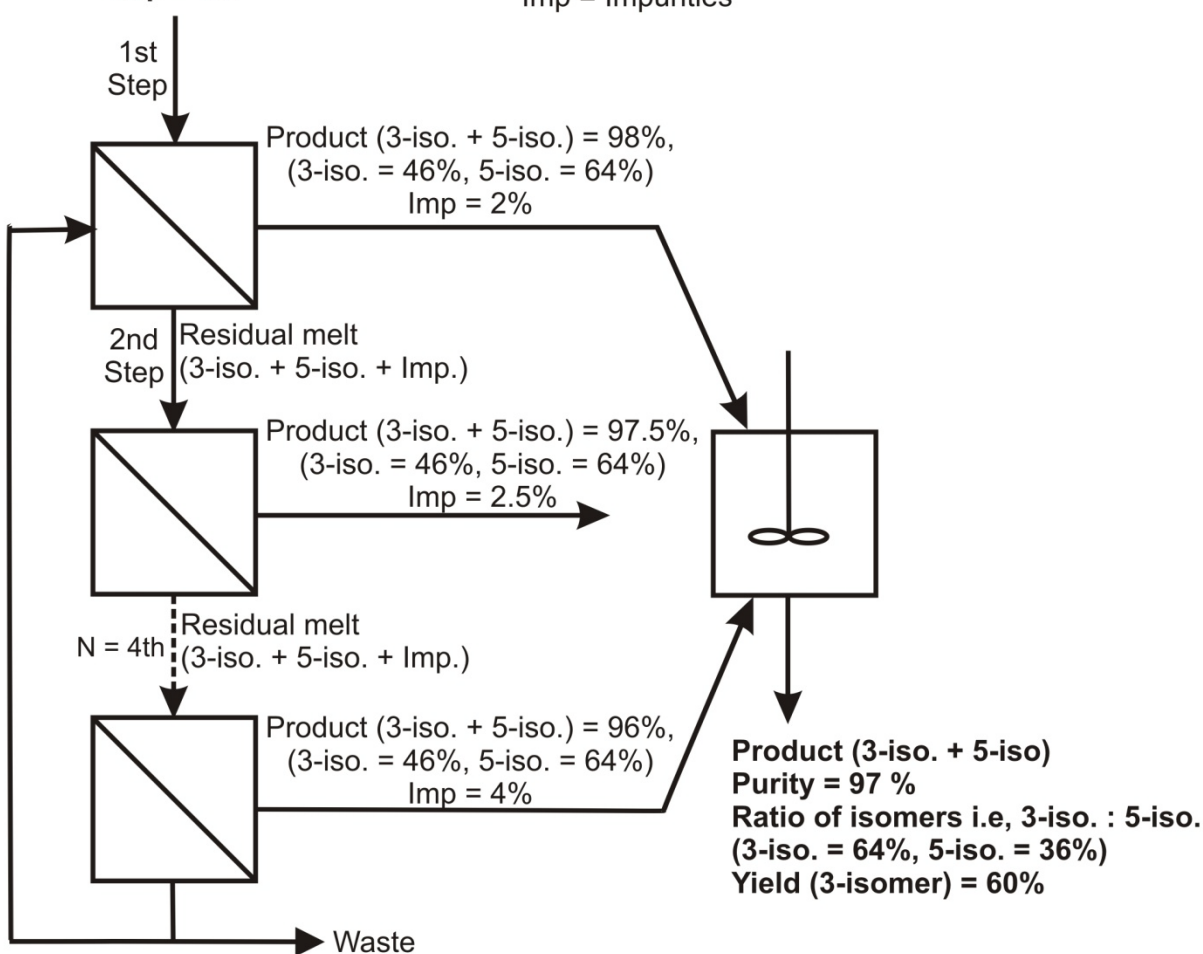


Fig. 6.2 Process flow diagram [Ahm15] [Ahm16]

6.1.7 Crystal Shape, habit and morphology

A single stable nuclei (a very small crystal) is isolated during the crystal growth of the melt and studied under the microscope to check the habit of crystal growth for 6 mins. A tetrahedral shape crystal forms in a supersaturated system and its size increases with a time to grow into a crystal of significant size as shown in Fig. 5.10. The crystal grows in size by the increase in the size of their faces. Normally they do maintain the geometric similarities and overlap with each other to form a layer. Due to the high supersaturation and high growth rate, these crystals grow in size quickly. In the beginning, at a low growth rate well-defined tetrahedral crystals are produced, but after 320 s the supersaturation of the melt increases and heat transfer effects dominate and dendritic morphologies appear on the surface of crystals [Ark95a] [Chi03]. This can be observed in Fig. 5.10 (g, h).

6.2 Case study II '3-isomer'

6.2.1 Solid-liquid equilibrium

To check the feasibility of separation of 3-isomer by layer melt crystallization, first solid-liquid binary phase diagram between 3-isomer and 5-isomer was measured. DSC was used to measure the solid-liquid phase diagram by taking the samples of different composition of 3 and 5-isomer. The DSC measurement shows an endothermic phase change at a constant temperature for all samples with different concentrations. This shows that a binary mixture of 3 and 5-isomer exhibit a binary eutectic system with a eutectic temperature of 88°C and the eutectic point at 0.01 wt.% of 5-isomer. This eutectic phase diagram can be seen in Fig. 5.11.

This result shows that 3-isomer and 5-isomer show a simple binary eutectic system and 3-isomer is a crystallizing compound which can be separated as a pure compound in a single step of melt crystallization.

6.2.2 Purity of the layer

This system is considered as a pure binary eutectic system in which the 3-isomer is taken as a pure component while all other components are considered as impurities.

The product composition is given in a Tab. 4.1. As discussed earlier the cooling rates affect the overall purity of the layer. At high cooling rates, the amount of impurity is high in the layer whereas at lower cooling rate process time is longer in other words operating cost is higher. Therefore, the purity of the layer is measured at medium cooling rates when the temperature of the cold finger at 65 °C. There is an increase in the purity of the layer after the crystallization. The purity of the layer is increased from 83% to the 87% in a single step of crystallization.

To further increase the purity of the layer an additional post-crystallization step a sweating is carried out. Sweating needs a much shorter retention time of about one hour only and is therefore faster compared to a crystallization process of 3 hours. In sweating, the temperature of the layer is raised near the melting point of the pure product which yields to a partial melting. This is due to the presence of impurities which lowers the melting point of the fractions. Due to this partial melting, the viscosity of the layer decreases and the amount of adhering impurities and inclusion is drained out under the influence of gravity. The final purity of the layer increased from 83% to 94% after sweating as shown in Fig. 5.12. There is an increase of 13% in the overall purity of 3-isomer after layer melt crystallization which is not possible in the distillation process.

Another important factor in the optimization of the sweating process is the yield of the process which is calculated by the percentage loss of the material during the sweating process. The percentage loss of the product calculated in this work is about 7% as shown in Fig. 5.12 which is according to the literature value [Ulr03b].

The ratio of the 3-isomer and the 5-isomer is also followed in the product by treating the residual melt in three different batches. Actually, in each case, the 3-isomer began to crystallize more and the ratio of 3-isomer is increased in the final product from 87% to 91%. This resulted in an increase of the overall purity of the product about 94% because in this case the 5-isomer is also taken as an impurity.

6.3 Energy efficiency of melt crystallization process

In the most used industrial applications of melt crystallization, batch wise crystallization on a cooled surface is used. The energy requirements of heating and cooling of the

whole crystallizer equipment, as well as the heat transfer medium, has to be taken into account. But in this work only the phase change energy of crystallization and distillation is used to calculate the energy demand and feasibility of the process by measuring the heat of fusion ΔH_{fus} and heat of vaporization ΔH_{vap} of the samples by DSC-TGA.

Normally the energy requirement for the melt crystallization is low in principle and strongly depends on process efficiency. The consumption of energy to crystalline or melt the crystal product for each stage is calculated in this work and with the help of heat of fusion and heat of vaporization. These values are calculated by using a DSC-TGA instrument and then related to the literature values to compare the process.

The value of phase transformation for crystallization is calculated by measuring the heat of fusion ΔH_{fus} and for distillation the heat of vaporization ΔH_{vap} is measured. All these values are given in Table 5.3 and are compared with each other. The heats of fusion for the majority of compounds with industrial importance are 2-5 times lower than the heats of vaporization [Wei94]. The lower energy demand can also be confirmed by the material used in this work. The values calculated for the heat of vaporization and heat of fusion of the product 'A' and 3-isomer are given in Table 5.3. The heat of vaporization for product 'A' is - 138 J/g and for 3-isomer it is - 139 J/g whereas the heat of fusion is - 610 [J/g] for product 'A' and - 453 [J/g] for 3-isomer respectively. These results are in total agreement with the literature values [Ark95b] as discussed earlier and heat of vaporization is 2 - 5 times lower in both cases.

On the basis heat of fusion and heat of vaporization, the phase transformation energies of both products are calculated and are given in Table 5.4. These phase energy values allow estimating the energy required to produce per gram of purified product by crystallization or distillation.

Melt crystallization has a high potential for energy saving compared to the conventional process like distillation due to the relatively low heat of phase transition. The energy difference between crystallization and distillation is found to be 78% for product 'A' and 69% for 3-isomer, as shown in Table 5.4. The values obtained above for the energy saving by melt crystallization for both compounds can be compared with values of

energy saving of other compounds presented by Verdoes and Arkenbout [Ver97] [Ulr04] in Tab. 6.1. It can be seen that 50 to 70 % of the energy demand of the process can be reduced by melt crystallization. This energy requirement can be reduced further by improving the heat integration. Wellinghoff and Wintermantel [Wel91] have also compared the energy consumption of distillation with that of crystallization. They found that the energy requirement of distillation corresponds to 1.2 to 4.0 times the heat of vaporization.

Tab. 6.1 Study of TNO for the Netherlands [Ver97] [Ulr04]

Component	Energy saving [%]
Caprolactam	50
Phenol	63
Dimethylterephthalate	96

6.4 Process flow diagram

The energy demand for each step process during crystallization is calculated only by measuring the phase change energies of the material during crystallization and vaporization by using DSC-TGA measurements as discussed in Chapter 5.3 and 5.3.2. These phase change energy values of vaporization and crystallization served as a source of energy balance of the process. The values of mass and energy demand calculated after each stage of crystallization are given in Tab. 6.2.

Tab. 6.2 Mass and energy demand calculated after each stage of crystallization

No. of stages	Amount of Product crystallized [g]	$Q = m\Delta H_{\text{melt.}}$ [KJ/h]
1	9.47	- 4.175
2	5.48	- 2.53
3	3.38	- 1.56
4	2.43	- 1.12

In the end a detailed description of the developed general process flow diagram of a complete process on the basis of the above discussion with complete mass and energy balance after each stage is shown in Fig. 6.3. This flow diagram can serve as the basis for successful process design at the industrial scale. The yield of the overall process is approximately 46% due to the limitation of lab scale layer melt crystallizer. The cold finger is used as a cooling surface for crystallization and less active area for crystallization is available. This is the main reason for the low yield of the process. But in commercially available crystallizer by Sulzer and Proabd, a large number of parallel plates are used as the cooling surface for the crystallization. The active surface area available for crysallization can be adjusted according to the process. This means high yield can be obtained in these industrial scale crystallizers.

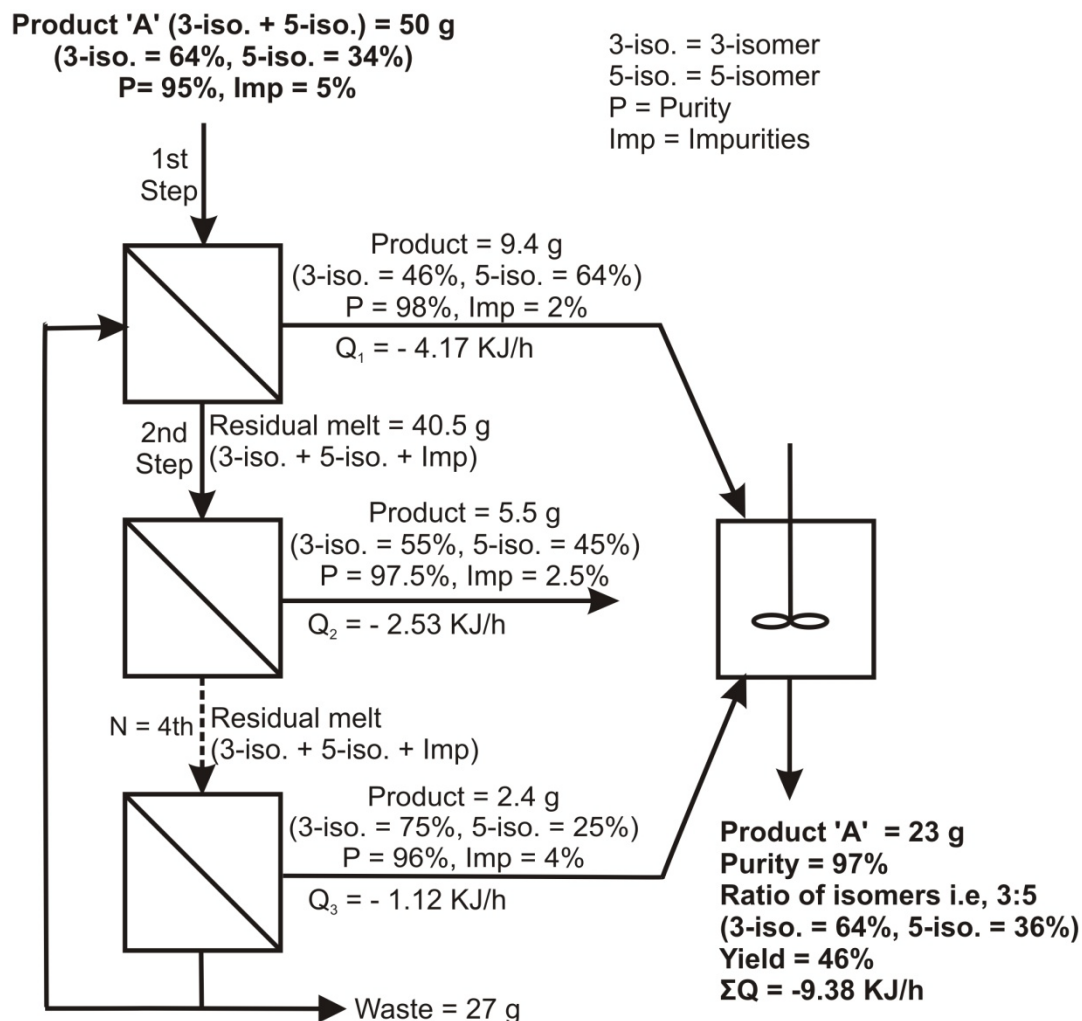


Fig. 6.3 Process flow diagram with mass and energy demand after each stage

7. Conclusion

After the consideration of the experimental result and discussion, the following conclusions can be drawn with regard to the aim outlined in Chapter 3.

- First, the respective melting point and heat of fusion data are used to calculate the values of liquidus lines by computing these values in the Schröder-van-Laar equation. After that thermal analysis through performing DSC measurements helped in determining the eutectic nature of the binary systems between product 'A' and 5-isomer. These results clearly show that this system is a simple binary eutectic with the eutectic point at a composition of 0.18 ± 0.01 wt.% and the eutectic temperature at 365 ± 3 K (91.85 °C). Eventually, the calculated and experimental values are compared with each other and they are found to be in good agreement with a standard deviation of approximately 5%.

It is clear from the results that this system is a simple binary eutectic system and can be separated in a single step of purification thermodynamically. The theoretical yield calculated by the phase diagram is found to be 78%.

- Afterward, the effect of cooling rates on crystal growth as a function of layer thickness is measured. The high cooling rates result in a fast increase in crystalline layer thickness followed by a decrease in crystal growth rate. It results in an increase in thermal conductive resistance of the crystalline layer due to an increase in thermal resistance of the layer and crystal growth rate decreases. Whereas a low cooling rate results in a slower growth rate and the layer needs a longer time to grow with a moderate increase in thermal resistances.

At fast cooling rates, the degree of supersaturation increases and the porous layer with high growth rate and concentration of the impurity is produced. Whereas at low cooling rates a compact structured layer is produced with the improved purity, but it takes longer operation times which are not favored due to the concerned economic reasons.

- To study the crystal morphology and habit of the product 'A' a single stable nuclei (a very small crystal) is isolated during the crystal growth of the melt and studied under the microscope. In the beginning, a well-defined tetrahedral crystal at low growth rate are produced. Its size increases with a time to grow into the crystals of significant size as shown in Fig. 5.10. After 320 s the supersaturation of the melt increases and heat transfer effects dominate and dendritic morphologies appear on the surface of the crystals.
- Conventionally, the product 'A' is being separated by vacuum distillation. However, the purification limit by distillation is 95% to date and cannot be further increased by distillation. These preliminary results for purity at different temperature of the cold finger show a good potential for the purification of the product by layer melt crystallization. Therefore, the process was further optimized for the better purification by using a combination of crystallization and sweating. The cooling rate at the cold finger of 65 °C was selected for the further investigation in this work. The sweating is a temperature induced purification step where the product is partially melted again with shorter retention time. The overall purity of the product was increased from 95 % to approximately 98% in a single step of crystallization and sweating. The yield of the process is also high with 8% loss of material during sweating.

The results show that the aim of the high purity of this product can be achieved by a combination of crystallization and sweating as compared to the distillation. Hence, melt crystallization can increase the purity to the level which is not achievable by distillation to date.

- The product is purified successfully by a single step of layer melt crystallization up to 98%, but the ratio of the two isomers is reversed after crystallization. To maintain the ratio of the 3 and 5-isomer in the product, an approach of treating the residual melt in different batches is used. The 3-isomer is separated from the 5-isomer in different batches and then all streams are mixed together to achieve the required product specifications. First to check the feasibility whether 3-isomer can be separated from the 5-isomer in the residual melt, the binary eutectic phase diagram was constructed

between 3 and 5-isomer. The yield calculated theoretically by the phase diagram was about 90%.

These results show a binary eutectic nature of the system with an eutectic point at a composition of 0.1 ± 0.03 wt. % and a eutectic temperature at approximately 88 °C.

- Hence, by this new strategy for the separation of the complex product with multi-components by simple melt crystallization is successfully achieved after four batches. In this method, one material was considered as a pure component and separated while others were considered as an impurity and treated later in a second crystallization stage just like a binary mixture system. By mixing all these fractions a product with the required specification can be produced with the maximum purity of about 97% (as compared to the purity obtained in a single step of crystallization which was 98%) and right mixture of the isomers. This means, to maintain the right mixture of the isomers, we have to compromise slightly on the purity.
 - In the case of the 3-isomer, the 3-isomer also show a eutectic behavior with the 5-isomer. The final purity of the layer was increased from 83% to 94% in a single step of purification by using a combination of crystallization and sweating. The percentage loss of the final product is about 7% after sweating, which is in an acceptable range.
 - Finally, the phase change energy of crystallization and distillation is used to calculate the energy demand and feasibility of the process. The energy difference between crystallization and distillation is found to be 78% for Product 'A' and 69% for the 3-isomer. In this way, energy requirement for the purification of these new products can be reduced to 50 to 70% by applying a layer melt crystallization process with combination post purification step of sweating compared to distillation.
- ➤ In conclusion, it can be accomplished that for higher purification demand for the complex feed streams in future the melt crystallization can be used as an alternative to distillation. It also increases the purity in a single step of purification to the level which is not achievable by distillation to date.

To maintain the ratio of the different components in the product, an approach of treating the residual melt was used. Thus, one component was separated from the other in different batches and then all streams were mixed together to achieve the required product specifications. Subsequently, this method has following benefits as compare to other unit operations. 1) It gives an alternative route for the separation of the complex mixture of the different material by separating them in different stages. 2) This method provides a degree of freedom to mix two different isomers together in different ratios which are more economically suited according to the situation and demand in the future. The overall yield of the process is also higher if there is no restriction of maintaining the product specification.

This method is also more economical and energy efficient compared to distillation as it operates at low temperatures, i.e., the melting point of material which is relatively low compared to the boiling points. The energy requirement for the melt crystallization is low in principle and strongly depends on process efficiency. The 50 to 70% of the energy demand of the process can be reduced by using the melt crystallization instead of distillation.

8. Summary

Melt crystallization can provide a unique solution with regard to high purity applications as well as environmental and health benefits. Melt crystallization is a highly selective and energy efficient method for the purification of the product. The application of layer melt crystallization processes is rapidly increasing in the field of separation of organic compounds. The layer melt crystallization process has an advantage of an easy scale up and an easy solid-liquid separation.

The aim of the work was to increase the purity of the new multi-component complex mixture of organic material to a level, which is to date not achievable by distillation as well as to keep the ratio of isomers constant in a final product to maintain the product quality.

In the first part of this work applicability of layer melt crystallization for separation of a complex feed streams product 'A' was evaluated. Normally, it is difficult to separate these multi-component products and appropriate procedures are required. The complex mixture of a product was taken as a case study which is an important technical product for an industry. It is a mixture of different components (isomers), some of which show eutectic behavior, while others are not and some impurities which decrease the overall purity of the product.

Here a new approach was adopted for the separation of multi-component products in order to keep the right ratio of the isomers as well as to increase the overall purity of the final product by reducing the amount of impurities. So during the experiments, one material was taken as a pure material and separated first, while others were taken as an impurity (as done so far, in order to have a binary component phase diagram). This "new" impurity is treated afterward again by a melt crystallization process.

For this purpose, first solid-liquid equilibria are measured for the complex mixture by using differential scanning calorimetry. The binary mixture of product 'A' and 5-isomer, show a simple binary eutectic phase diagram with the eutectic point at a composition of 0.18 ± 0.01 wt.% and the eutectic temperature at 365 ± 3 K (91.85 °C). Afterward, on

the basis of this information different experiments were carried out on a laboratory-scale layer melt crystallizer. First, the purification of a complex feed stream by melt crystallization was measured by studying different optimization parameters like crystal growth rate, crystallization time and purity. The product was successfully purified by a single step of layer melt crystallization from 95% up to 98%. After that in a second step, the desired composition of the final product (64% of the 3-isomer and 36% of the 5-isomer) was achieved by adding components resulting from the different stage of crystallization since the first crystallization gave only the desired purity, but did not give the right mixture of the two isomers in the product. The approach found to be successful for the purification of complex feed streams.

In the second part, the 3-isomer was taken as a case study which is also an important industrial product and the main constituent of the product 'A'. This system was measured as a pure binary eutectic system whereby 3-isomer was considered as a pure component while other components were considered as impurities. Therefore, to check the feasibility of the layer melt crystallization process first a binary eutectic phase diagram was constructed between the 3 and 5-isomer. In this case, 3 and 5-isomer also show the eutectic behavior with the eutectic point at a composition of 0.1 ± 0.03 wt.% and the final purity of the 3-isomer was increased from 83% to 94%.

At the end, the phase transformation energy of crystallization and distillation was used to calculate the energy demand of both processes by measuring the heat of fusion ΔH_{fus} and the heat of vaporization ΔH_{vap} of the samples. These values were measured by using a DSC-TGA. The energy demand calculated by the heat of fusion and heat of vaporization was compared together. The energy requirement for this new product can be reduced from 50 to 70% by applying the layer melt crystallization.

On the basis of above discussion, the process flow diagram of a complete process based on mass and energy balance after each stage was constructed conclusively. This flow diagram provides complete information about the ratio of 3 and 5-isomer with their purity after every stage. This flow diagram can serve as the basis for successful process design at the industrial scale.

9. Zusammenfassung

Die Schmelzkristallisation ist ein hochselektives und effizientes Aufreinigungsverfahren, das sich besonders für die Herstellung hochreiner Produkte unter Berücksichtigung entsprechender Umwelt- und Gesundheitsaspekte eignet. Dabei verzeichnet insbesondere die Schichtkristallisation ein stark wachsendes Interesse im Bereich der Auftrennung organischer Substanzen. Zusätzliche Vorteile der Schichtkristallisation bestehen in einem einfachen Scale-up sowie einer einfachen Fest-Flüssig-Trennung.

Das Ziel dieser Arbeit besteht darin, die Reinheit eines neuen Multikomponentensystems bestehend aus organischen Substanzen auf einen Wert zu erhöhen, der durch konventionelle Destillation nicht zu erreichen ist. Dies soll unter der Maßgabe der Aufrechterhaltung des Isomerverhältnisses im Endprodukt erfolgen, um eine entsprechende Produktqualität zu gewährleisten.

Im ersten Teil der vorliegenden Arbeit wurde die generelle Anwendbarkeit der Schichtkristallisation hinsichtlich der Trennung des komplexen Stoffgemisches „A“ im Rahmen einer Fallstudie untersucht, bei dem es sich um ein bedeutsames technisches Produkt handelt. Das Stoffgemisch besteht aus verschiedenen Komponenten (Isomeren), wovon einige ein eutektisches Verhalten zeigen und wiederum andere entsprechende Verunreinigungen darstellen, die die Reinheit des Produktes entsprechend verringern.

Ein neuer Ansatz für die Trennung eines Multikomponentensystems wurde vorgestellt und angewandt, der zum einen die korrekte Verteilung der Isomere gewährleistet und zum anderen die Reinheit des Endproduktes durch die Verringerung der enthaltenen Verunreinigungen deutlich erhöht. Im Rahmen der experimentellen Untersuchungen wurde ein Material in reiner Form abgetrennt, während die anderen als Verunreinigungen behandelt wurden. Diese „neuen“ Verunreinigungen wurden nachträglich erneut durch Schmelzkristallisationsprozesse aufgetrennt.

Zu diesem Zweck wurde zunächst das Fest-Flüssig-Equilibrium des komplexen Multikomponentensystems durch dynamische Differenzkalorimetrie (DSC) bestimmt. Das binäre Gemisch bestehend aus Produkt „A“ und 5-Isomer zeigte ein einfaches binäres eutektisches Phasenverhalten, wobei der eutektische Punkt bei einer Zusammensetzung von 0.18 ± 0.01 wt.% und einer Temperatur von 365 ± 3 K (91.85 °C) zu finden ist.

Auf Basis dieser Daten erfolgte die Durchführung von Experimenten mithilfe eines Laborkristallisators, mit dem Ziel die Kristallwachstumsgeschwindigkeiten sowie die entsprechenden Reinheit und Ausbeuten unter dem Einfluss variierender Kristallisationszeiten und -temperaturen als Funktion der Schichtdicke zu bestimmen. Das Produkt konnte erfolgreich in einem Schichtkristallisationsschritt von 95 auf 98% aufgereinigt werden. In einem zweiten Verfahrensschritt konnte die geforderte Zusammensetzung des Endproduktes (64% 3-Isomer und 36% 5-Isomer) durch die Zugabe zusätzlicher Komponenten erreicht werden, die aus verschiedenen Stufen der Schichtkristallisationen des jeweiligen Rückstandes entstammten. Dieser Ansatz erwies sich als erfolgreich für die Aufreinigung komplexer Mehrkomponentensysteme mit der zusätzlichen Randbedingung, dass die verbleibenden Komponenten ein bestimmtes Mischungsverhältnis aufweisen müssen.

Im zweiten Teil der Arbeit wurde das 3-Isomer im Rahmen einer Fallstudie untersucht, das ebenfalls als ein bedeutendes industrielles Produkt als Hauptbestandteil im Produkt „A“ enthalten ist. Das zu untersuchende System wurde als reines binäres eutektisches System betrachtet, bei dem das 3-Isomer als Zielkomponente definiert wurde, während die anderen enthaltenen Komponenten entsprechend die Verunreinigungen darstellen. Um die Durchführbarkeit einer Schichtkristallisation zu untersuchen wurde zunächst ein binäres eutektisches Phasendiagramm mit dem 3- und 5-Isomer konstruiert. Auch in diesem Fall zeigten 3- und 5-Isomer ein eutektisches Verhalten mit dem entsprechenden eutektischen Punkt bei der Zusammensetzung von 0.1 ± 0.03 wt.%. Die Reinheit des 3-Isomers konnte dabei von 83% auf 94% erhöht werden.

Abschließend wurden die Phasenumwandlungsenergien von Kristallisation und Destillation herangezogen, um den jeweiligen Energiebedarf beider Prozesse durch die Bestimmung von Schmelzwärme ΔH_{fus} Verdampfungswärme ΔH_{vap} der Proben miteinander zu vergleichen. Die dafür benötigten Größen wurden mittels DSC-TGA bestimmt. Dabei konnte festgestellt werden, dass der Energiebedarf bei Anwendung des Schichtkristallisationsverfahrens um 50 bis 70% im Vergleich zur Destillation reduziert werden konnte.

Auf der Basis der gewonnenen Daten und Ergebnisse wurde auf Basis einer Massen- und Energiebilanzierung nach jedem Prozessschritt ein Fließschema des gesamten Prozesses entwickelt und dargestellt. Das Fließschema beinhaltet die vollständigen Informationen über das Verhältnis von 3- und 5-Isomer und der entsprechenden Reinheit nach jedem Prozessschritt und kann als Basis für ein erfolgreiches Produktdesign in industriellen Maßstäben dienen.

10. List of symbols and abbreviations

Latin Symbols

A	[%]	Ratio of 3-isomer
B	[%]	Ratio of 5-isomer
Imp	[%]	Amount of impurities
ΔL	[mm]	Thickness of crystal layer
P	[Pa]	Vapor pressure
P_0	[Pa]	Standard vapor pressure at 25°C
Q	[J/g]	Phase change energy
T_A	[°C]	Temperature of component A
T_{eq}	[°C]	Temperature at equilibrium
T_m	[°C]	Melting temperature
T	[°C]	Temperature
ΔT	[°C]	Degree of supersaturation
Δt	[sec]	Time interval
ΔH_m	[J/mol]	Molar heat of fusion
ΔH_{fus}	[J/g]	Heat of fusion
ΔH_{vap}	[J/g]	Heat of vaporization
ΔH_{Sub}	[J/g]	Heat of sublimation
R	[J/K mol]	Real gas constant
v/v %	[%]	Volume percent
wt. %	[%]	Weight percent
x_F	[%]	Concentration of feed

x_{EP}	[%]	Concentration at eutectic point
x_i	[-]	mole fraction
X_i	[mol/L]	molar concentration
Y	[%]	Yield of the process

Greek symbols

μ_i^L	[J/mol]	Chemical potential of liquid
μ_i^S	[J/mol]	Chemical potential of solid
μ_{i0}^L	[J/mol]	Standard Chemical potential
δ_{mass}	[m]	Mass boundary layer
δ_{Heat}	[m]	Heat boundary layer

Abbreviations

DSC	Differential scanning calorimetry
eu	Eutectic point
HPLC	High performance liquid chromatography
L	Liquid
S	Solid
TGA	Thermal gravimetric analysis

11. References

- [Ahm16] M. Ahmad, J. Ulrich: Separation of complex feed streams of products by layer melt crystallization, *Chem. Eng. Tech.*, 39 (2016) 7, 1341-1345.
- [Ahm15] M. Ahmad, J. Ulrich: Separation of complex feed streams of products by layer melt crystallization, in *Proc. of 22nd BIWIC*, Eds.: K. J. Kim, K. Lee, Daejeon, South Korea, 2015, 237-244.
- [Ark95] G. F. Arkenbout: *Melt Crystallization Technology*, Technomic Publishing Company, Lancaster, 1995.
- [Ark95a] G. F. Arkenbout: Thermodynamics limits, in *Melt Crystallization Technology*, Technomic Publishing Company, Lancaster, 1995, 57-83.
- [Ark95b] G. F. Arkenbout: Prospect of Melt Crystallization, in *Melt Crystallization Technology*, Technomic Publishing Company, Lancaster, 1995, 03-18.
- [Bei12] T. Beierling, A. Ruether: Separation of the isomeric long chain aldehydes dodecanal/2-methylundecanal via layer melt crystallization, *Chem. Eng. Sci.*, 77 (2012), 71-77.
- [Bei13] T. Beierling, J. Osiander, G. Sadowski: Melt Crystallization of isomeric long-chain aldehydes from hydroformylation, *Sep. and Purif. Tech.*, 118 (2013), 13-24.
- [Bra86] J. L. Bravo, J. R. Fair, J. L. Humphery: *Fluid mixtures separation technologies for cost reduction and process improvement*, Noyes Publications, New Jersey, 1986, 216-237.
- [Bro97] P. Brown, K. De Antonois: High Performance Liquid Chromatography, in *Handbook of Instrumental Techniques for Analytical Chemistry*, Ed.: F. Settle, Prentice Hall, New Jersey, 1997, 147-164.
- [Cam10] L. Campanella, V. Micieli, M. Tomassetti, S. Vecchio: Solid-liquid phase diagram of binary mixtures, *J. Therm. Anal. Cal.*, 99 (2010), 887-892.

- [Cha10] K. Chaleepa: A New Concept in Layer-Based Fractional Crystallization Processes for Fats, PhD Thesis, Center for Engineering Sciences, Martin-Luther-Universität Halle-Wittenberg, 2010.
- [Chi03] A. Chianese, M. Parisi: Kinetics: Fundamental of Nucleation and Crystal growth, in Melt Crystallization Fundamentals, Equipment and Applications, Eds.: J. Ulrich, H. Glade, Shaker Verlag, Aachen, 2003, 41-69.
- [Gab08] P. Gabbott: A Practical Introduction to Differential Scanning Calorimetry, in Principles and Applications of Thermal Analysis, Ed.: P. Gabbott, Blackwell Publishing Ltd, Oxford, 2008.
- [Gil91] S. W. Gilbert: Melt crystallization: Process analysis and optimization, AIChE Journal, 37 (1991) 8, 1205-1218.
- [Gla03] H. Glade, J. Ulrich: Laboratory tests for Melt Crystallization, in Melt Crystallization Fundamentals, Equipment and Applications, Eds.: J. Ulrich, H. Glade, Shaker Verlag, Aachen, 2003, 129-162.
- [Hen10] A. Hengstermann: A new approach to industrial melt crystallization of acrylic acid, PhD Thesis, Delft University of Technology, Shaker Verlag, Aachen, 2010.
- [Jan87] S. J. Jancic: Fractional crystallization, In Pro. of the 10th Symposium on Industrial Crystallization, Bechyne, 1 (1987), 57-70.
- [Jan94] P. J. Jansens, G. M. van Rosmalen: Fractional Crystallization. in Handbook of Crystal growth, Vol 2, Ed.: D. T. J. Hurle, Elsevier Science B.V., Amsterdam, 1994, 289-314.
- [Kim01] K. J. Kim, J. Ulrich: Purification of crystalline layer by controlling the temperature gradient, Powder Tec., 121 (2001), 81-87.
- [Kim02] K. J. Kim, J. Ulrich: A quantitative estimation of purity and yield of crystalline layers concerning sweating operation, J. of Crys. Gro., 234 (2002) 2/3, 551-560.

- [Kim03] K. Kim, S.H. Lee, J. Ulrich: Experimental thermal conductivity of ice crystalline layer in layer melt crystallization, *J. Ind. Eng. Chem.*, 9 (2003), 111-116.
- [Kön03] A. König: Phase diagrams: in *Melt crystallization, Fundamentals, Equipment and Applications*, Eds.: J. Ulrich, H. Glade, Shaker Verlag, Aachen, 2003, 7-40.
- [Kön08] A. König, M. Stepanski, A. Kuszlik, P. Keil, C. Weller: Ultra-purification of ionic liquids by melt crystallization, *Chem. Eng. Res. & Des.*, 86 (2008) 7, 775-780.
- [Mat77] M. Matsuoka: Solid liquid phase equilibria of binary organic mixtures, *Sep. Pro. Eng.*, 7 (1977), 245-249.
- [Moh02] R. Mohan, H. Lorenz, A. S. Myerson: Solubility Measurement Using Differential Scanning Calorimetry, *Ind. Eng. Chem. Res.*, 41 (2002), 4854-4862.
- [Nie95] S. Niehörster, J. Ulrich: Designing Crystal Morphology by a Simple Approach, *Cryst. Res. Tech.*, 30 (1995), 389-395.
- [Pet07] R. H. Petrucci, W. S. Harwood, F. G. Herring, J. D. Madura: *General Chemistry: Principles & Modern Applications*. 9th ed. Prentice Hall Publication, New Jersey, 2007, 242-248.
- [San94] N. Santilli, P. D. Filippis, A. Chianese: Solid- Liquid Phase Diagram of the Binary System Benzil + 2,2-Dimethoxy-1, 2-Diphenylethanone, *J. Chem. Eng.*, 39 (1994), 179-180.
- [Sau09] S. Sauerbrunn, M. Zemo: Measuring the heat of evaporation by TGA/DSC, *American laboratory*, Jan. 15, 2016.
- [Sch93] R. Scholz, K. Wangnick, J. Ulrich: On the distribution and movement of impurities in crystalline layers in melt crystallization processes, *J. Phys. D: Appl Phys*, 26 (1993), B156-B161.

- [Sha12] C. Shan, L. Xingang, W. Jun. X. Changchun: Optimization of Parameters for Melt Crystallization of P-Cesrol, *Chinese Journal of Chem. Eng.*, 20 (2012) 4, 649-653.
- [Shi93] H. Shibuya, Y. Suzuki, K. Yamaguchi, K. Arai, S. Saito: Measurement and prediction of solid liquid equilibria of organic compound mixture, *Fluid Phase Equil.* 82 (1993), 397-405.
- [Shr12] A. Shrivastava, V. B. Gupta: HPLC: Isocratic or Gradient Elution and Assessment of Linearity In Analytical Methods, *J. Adv. Sci. Res.*, 3 (2012) 2, 12-20.
- [Sil04] R. de Silva, L. Santos, B. Schroder, O. Fernandes: Measurement of enthalpies of sublimation by drop method in a cavity type calorimeter: design and test of a new system, *J. Therm. Acta.*, 415 (2004), 15-20.
- [Sin12] M. R. Singh, J. Chakraborty, N. Nere, H. Tung, S. Bordawekar, D. Ramkrishna: Image-Analysis-Based method for 3D crystal morphology measurement and polymorph identification using confocal microscopy, *Cryst. Growth Des.*, 12 (2012), 3735–3748.
- [Sko98] A. Skoog., C. Holler, B. Nieman: Principles of Instrumental Analysis, 5th Ed. Saunders College Publishing, 1998, 673-697 and 725-766.
- [Sla95] D. W. Slaughter, M. F. Doherty: Calculation of solid-liquid equilibrium and crystallization paths for melt crystallization processes, *Chem. Eng. Sci.*, 50 (1995) 11, 1679-1694.
- [Ste03] M. Stepanski, E. Schäfer: Separate organics by melt crystallization: A guide to when and how to use this technique, in *Melt crystallization: Fundamentals, Equipment and Applications*, Eds.: J. Ulrich, H. Glade, Shaker Verlag, Aachen, 2003, 167-189.
- [Tak02] H. Takiyama, H. Suzuki, H. Uchida, M. Matsuoka: Determination of solid liquid phase equilibria by using measured DSC curves, *Fluid Phase Equilibria*, 194–197 (2002), 1107-1117.

- [Tau09] P. Taulelle, G. Sitja, G. Pepe, E. Garcia, C. Hoff, S. Veessler: Measuring Enthalpy of Sublimation for Active Pharmaceutical Ingredients: Validate Crystal Energy and Predict Crystal Habit, *Cry. Growth & Design*, 9 (2009), 4706-4709.
- [Ulr96] J. Ulrich, J. Bierwirth, S. Henning: Solid layer melt crystallization, *Separation and purification methods*, 25 (1996) 1, 1-45.
- [Ulr02] J. Ulrich, H: C. Bülau: Melt crystallization, in *Hand book of Industrial Crystallization*, Ed.: A. S. Myerson, 2nd ed., Boston, Butterworth-Heinemann, 2002, 161-177.
- [Ulr03] J. Ulrich: Melt crystallization: Fundamentals, Equipment and Applications, Ed.: J. Ulrich, H. Glade, Shaker Verlag, Aachen, 2003.
- [Ulr03a] J. Ulrich: Introduction, Melt crystallization: in *Fundamentals, Equipment and Applications*, Ed.: J. Ulrich, H. Glade, Shaker Verlag, Aachen, 2003, 1-5.
- [Ulr03b] J. Ulrich: Solid layer Crystallization, in *Fundamentals, Equipment and Applications*, Ed.: J. Ulrich, H. Glade, Shaker Verlag, Aachen, 2003, 71-92.
- [Ulr04] J. Ulrich: Is Melt Crystallization a Green Technology, *Crys. Gro. and Des.*, 4 (2004) 5, 879-880.
- [Ulr11] J. Ulrich, S. Nordhoff: Schmelzkristallisation, in *Fluidverfahrentechnik. Grundlagen, Methodik, Technik, Praxis*, Ed.: H. R. Goedecke, Willey-VCH Verlag GmbH & Co. KGaA, 2011, 1131-1196.
- [Ulr13] J. Ulrich, T. Stelzer: Melt Crystallization, in *Crystallization Basic Concepts and Industrial Applications*, Ed.: W. Beckmann, Wiley-VCH Verlag GmbH, 2013, 289-304.
- [Ver97] D. Verdoes, G. J. Arkenbout, O. S. L. Bruinsma; P. G. Koutsoukos, J. Ulrich: Improved procedures for separating crystals from the melt, *Appl. Therm. Eng.* 17 (1997) 8-10, 879-888.

- [Wel91] G. Wellinghoff, K. Wintermantel: Schmelzkristallisation-theoretische Voraussetzungen und technische Grenzen. Chemie Ingenieur Technik, 63 (1991) 9, 881-891.
- [Wel94] G. Wellinghoff, K. Wintermantel: Melt crystallization: theoretical premises and technical limitations, Inter. Chem. Eng. 34 (1994) 1, 17-27.

Declaration

Hereby, I Muhammad Ahmad, certify that the presented thesis work titled “**Separation of complex feed streams of products by layer melt crystallization**” was done by me or students under my supervision. Materials obtained from other sources have been duly acknowledged and cited in the thesis. This work has not been previously presented in identical or similar form to any other German or foreign universities and institutes. This thesis work was conducted from 2013 to 2016 in Center of engineering sciences, Chair of thermal process engineering (TVT), Martin Luther University Halle-Wittenberg.

Muhammad Ahmad

Halle (Saale), 21.07.2016

Selbständigkeitserklärung

Ich versichere hiermit ehrenwörtlich, dass ich die vorliegende Arbeit mit dem Titel **„Separation of complex feed streams of products by layer melt crystallization“** selbstständig und nur unter Benutzung der angegebenen Literatur und Hilfsmittel angefertigt habe.

Die aus fremden Quellen direkt oder indirekt übernommenen Stellen sind als solche kenntlich gemacht und werden in der Arbeit aufgeführt.

Die Arbeit hat in gleicher oder ähnlicher Form noch keiner Prüfungsbehörde vorgelegen.

Ahmad, Muhammad

Halle (Saale), 21.07.2016

Curriculum vitae

Personal Information:

Name Ahmad, Muhamamd
Address Brandbergweg 35,
06120 Halle (Saale), Germany
Date of birth 23.08.1983
e-mail muhammad.ahmad@iw.uni-halle.de

Qualification:

PhD - student Chair of Thermal Process Engineering (TVT),
Martin Luther University Halle-Wittenberg, Germany
(Since 01.02.2013)

Master Master study of Chemical and Process Engineering,
Otto-von-Guericke University Magdeburg, Germany

Bachelor Bachelor of Science in Chemical Engineering,
Bahauddin Zakariya University Multan, Pakistan

Work Experience:

06/2009 - 03/2010 Max Planck Institut für Dynamic Komplexer Technischer
Systeme, Magdeburg-Germany

10/2007 - 10/2008 Department of Chemical Engineering
Comsat Institute of Information and Technology,
Lahore-Pakistan

Publications:

- M. Ahmad, J.Ulrich: Separation of complex feed streams of product by layer melt crystallization, Chem. Eng. Tech., 39 (2016) 7, 1341-1345.
- M. Ahmad, J.Ulrich: Separation of complex feed streams of product by layer melt crystallization, in 22nd proceedings of BIWIC 2015, Eds.: K. J. Kim, K. Lee, Daejeon, South Korea, 2015, 237-244.

Halle (Saale)

Muhammad Ahmad